AD-A079 625 HUGHES RESEARCH LABS MALIBU CA F/G 20/6
FIBER OPTIC COUPLERS.(U)
NOV 79 C K ASAWA F19628-78-C-0201
UNCLASSIFIED RADC-TR-79-263 NL

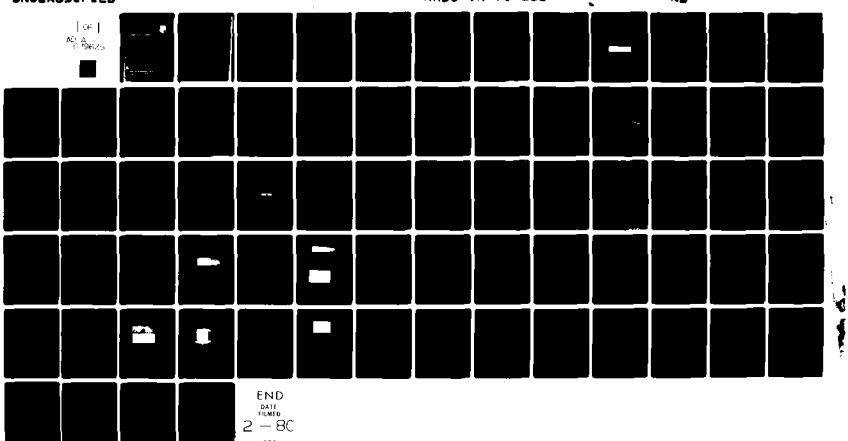

END
DATE FILMED
2 — 80
DDC

LEVEL II

RADC-TR-79-263
Interim Report
November 1979

FIBER OPTIC COUPLERS

Hughes Research Laboratories

C. K. Asawa

ROME AIR DEVELOPMENT CENTER
Air Force Systems Command
Griffiss Air Force Base, New York 13441

This report has been reviewed by the RADC Public Affairs Office (PA) and is releasable to the National Technical Information Service (NTIS). At NTIS it will be releasable to the general public, including foreign nations.

RADC-TR-79-263 has been reviewed and is approved for publication.

APPROVED: Richard Payne

RICHARD PAYNE
Project Engineer

APPROVED: Clarence D. Turner

CLARENCE D. TURNER
Acting Director
Solid State Sciences Division

FOR THE COMMANDER: John P. Huss

JOHN P. HUSS
Acting Chief, Plans Offic

If your address has changed or if you wish to be removed from the RADC mailing list, or if the addressee is no longer employed by your organization, please notify RADC (ESO), Hanscom AFB MA 01731. This will assist us in maintaining a current mailing list.

Do not return this copy. Retain or destroy.

UNCLASSIFIED

SECURITY CLASSIFICATION OF THIS PAGE (When Data Entered)

(19) REPORT DOCUMENTATION PAGE		READ INSTRUCTIONS BEFORE COMPLETING FORM
(18) 1. REPORT NUMBER: RADC-TR-79-263	2. GOVT ACCESSION NO.	3. RECIPIENT'S CATALOG NUMBER
(6) 4. TITLE (and Subtitle): FIBER OPTIC COUPLERS.		(9) 5. TYPE OF REPORT & PERIOD COVERED: Interim Report. 1 Aug 78 — 31 May 79
		6. PERFORMING ORG. REPORT NUMBER: N/A
(10) 7. AUTHOR(s): C. K. Asawa		(15) 8. CONTRACT OR GRANT NUMBER(s): F19628-78-C-0201
9. PERFORMING ORGANIZATION NAME AND ADDRESS: Hughes Research Laboratories, 3011 Malibu Canyon Road, Malibu CA 90265		(16) 10. PROGRAM ELEMENT, PROJECT, TASK AREA & WORK UNIT NUMBERS: 62702F 4600 1925 (17) 19
11. CONTROLLING OFFICE NAME AND ADDRESS: Deputy for Electronic Technology (RADC/ESO), Hanscom AFB MA 01731		(11) 12. REPORT DATE: November 1979
		13. NUMBER OF PAGES: 75
14. MONITORING AGENCY NAME & ADDRESS (if different from Controlling Office): Same (12) 74		15. SECURITY CLASS. (of this report): UNCLASSIFIED
		15a. DECLASSIFICATION/DOWNGRADING SCHEDULE: N/A

16. DISTRIBUTION STATEMENT (of this Report)

Approved for public release; distribution unlimited.

17. DISTRIBUTION STATEMENT (of the abstract entered in Block 20, if different from Report)

Same

18. SUPPLEMENTARY NOTES

RADC Project Engineer: Richard Payne (RADC/ESO)

19. KEY WORDS (Continue on reverse side if necessary and identify by block number)

Planar couplers
Ion exchange waveguides
Field assisted ion exchange

20. ABSTRACT (Continue on reverse side if necessary and identify by block number)

The purpose of this contract is to conduct research and development of new fabrication techniques for couplers for use with single strand multimode optical fiber waveguides.

The structures investigated BY near this contract were directional couplers and 8 (x) 8 planar transmission star couplers BY. Both theoretical and experimental characterization of the 8 (x) 8 transmission couplers were made. The waveguide → over
(Cont'd)

DD FORM 1 JAN 73 1473

UNCLASSIFIED

SECURITY CLASSIFICATION OF THIS PAGE (When Data Entered)

172,690

Item 20 (Cont'd)

structures were fabricated on a Nd-rich glass substrate using an ion-exchange process. The structure patterns were formed on the substrate by means of photolithography. Limited experiments demonstrating the fabrication of thick films by chemical vapor deposition on silica were also performed.

The initial part of this report summarizes the R&D effort between 1 April 1979 to 31 May 1979. The remainder of the report covers the effort between 1 August 1978 to 31 May 1979 and is divided into four bimonthly segments.

TABLE OF CONTENTS

PREFACE

This interim technical report covers the R&D performed by the Hughes Research Laboratories under the contract entitled "Fiber Optic Couplers", contract number F19628-78-C-0201, with RADC-ESO, over the period 1 August 1978 to 31 May 1979. The program manager is Dr. M.K. Barnoski and the principal investigator is Dr. C.K. Asawa. Program contributors are: Dr. O.G. Ramer, Dr. G.L. Tangonan, Mr. D.L. Persechini, Ms. L.E. Gorre, and Mr. H.R. Friedrich.

SECTION 1

R&D PERIOD, 1 APRIL 1979 TO 31 MAY 1979

During the fifth bimonthly period the effort was directed towards forming buried channel waveguides, (1) by fusing and laminating two planar waveguides and (2) by forming deep channel waveguides by means of electric field assisted ion exchange. The latter is a first step in a double ion exchange process to form buried waveguides of sufficiently high numerical aperture.

FUSED BURIED WAVEGUIDES

A small effort was expended to examine the potential for forming circularly symmetric buried channel waveguide by laminating two matching, shallow planar waveguides and then fusing the two waveguides by applying pressure and temperature. The results were not particularly encouraging as a method for forming fine-structured waveguides. Problem areas are described here briefly.

Several 10 cm^2 window glass samples in layered pairs were inserted into an oven, and varying pressures from 0 to 10 N/cm^2 were applied to the layers. The temperature of the oven was raised to 700°C, held there for 5 minutes, and then lowered to room temperature. The results were that (1) each sample "wet" or fused together; (2) the samples with the highest pressure (~10 N/cm^2) were distorted in shape; (3) air was entrapped at the interfaces for all samples. We found subsequently that lower temperatures (~600°C) over a 5 minute period were sufficient to wet the two layers of glass. Air entrapment between the layers still remained a problem. A vacuum oven was expected to solve the latter problem.

Before proceeding further with the measurement of fusion temperature-pressure relationship, we decided that an examination of the waveguide characteristics subsequent to these processing temperatures and time intervals was warranted. We found that a set of narrow, adjacent channel waveguides submitted to these temperatures and time intervals were completely diffused. The individual channels no longer existed, having diffused with the other channels into a planar waveguide.

It is possible that lower temperature and time intervals for fusing can be attained. However, the refractive index difference between the channel and the substrate is initially low ($\Delta n \sim 0.009$); further temperature time processing will further decrease the index difference, resulting in an inferior waveguide. Therefore, the high temperature fusing experiment was discontinued.

PRESSURE AND ADHESIVE LAMINATED BURIED CHANNELS

Further experiments on laminating two ion-diffused planar guides to form nearly circularly symmetric, buried channel waveguides were initiated. By pressing two waveguides together, we have demonstrated a "buried" 8 x 8 transmission star coupler. A second experiment, where the two planar guides are glued together, was performed. These experiments are described here.

Fig.1a shows how the laminate of matched 8 x 8 transmission star waveguide was prepared. The guides were pressed together with clamps, with channels on both ends registered. The sides of the glass substrates were then epoxied as shown; after the epoxy was cured, the mechanical

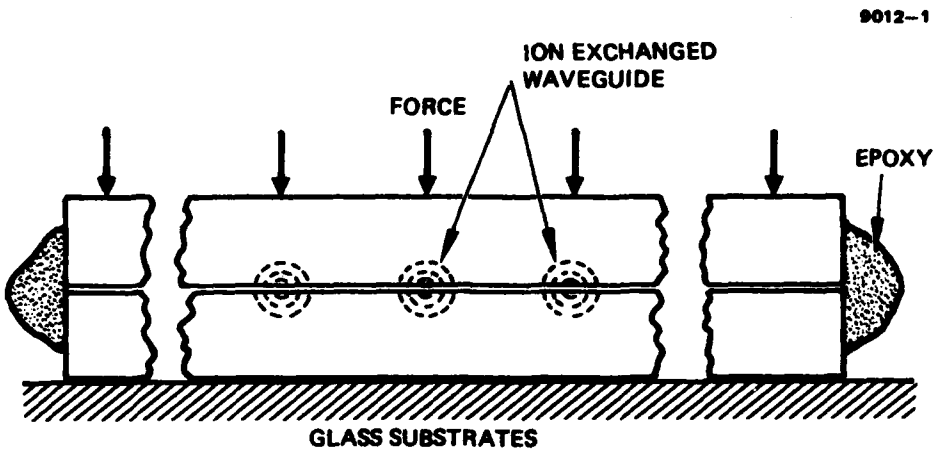

(a)

(b)

Figure 1. Buried channels lamination formed by pressure and cementing edges.
(a) Schematic of construction.
(b) 8 x 8 transmission star coupler.

clamps were removed. Figure 1b shows the near field output pattern when one of the 8 input ports was excited by 6328 Å light from a graded index fiber. A thin dark line appears in the pattern of Fig. 1b corresponding to an air gap between the two guides.

The throughput efficiency of the pressure laminated waveguide was approximately that of a single ion-exchange 8 x 8 waveguide described in the previous report. The lack of improved throughput efficiency is not of concern since the starting waveguide had an ion-exchanged area much larger than that of the fiber core. (We did not examine the optical characteristics any further, directing our efforts towards gluing the laminates and the electric field ion exchange experiments described below.)

The lamination of the two waveguides has proved to be non-trivial. One of the problems has been that the glass substrate is considerably distorted by the ion exchange process due to volume shrinkage of the Li-rich glass. A solution has been to form matching waveguides on either side of the glass substrate as described in the previous report. The result has been a substrate that is nominally uniform (within $\sim$1 mm) over a 1 x 4 inch glass plate.

A further problem has been that the surface over the ion diffused region is submerged $\sim$2 μm below that of the substrate. Optical polishing of the surface is necessary to form the laminate. However, the 1 mm fluctuation of the surface from flatness precludes polishing of the glass in that state since the waveguide is $\sim$0.1 mm in depth; part of the waveguide would be removed in polishing. We have developed a technique for "flattening" the glass substrate in preparation for polishing. The glass substrate is waxed onto an optical flat with the waveguide surface

facing the optically flat surface. Low temperature wax is used. The upper surface of the substrate is then waxes to a flat surfaced holder with high temperature wax. The holder is firmly pressed against the substrate and optical flat as the high temperature wax solidifies. The holder-substrate assembly is then removed for the optical flat by melting the low temperature wax. The waveguide surface can then be uniformly polished.

Besides using pressure plus epoxy on the edges to form laminates, we have glued two polished waveguides together with Eastman 910. Unfortunately we have broken two pairs of waveguides during the clamping process thus far. The clamping procedure is being rectified and will be used to continue the study of glued waveguide laminates.

FORMATION OF ELECTRIC FIELD ASSISTED WAVEGUIDES

In order to form usable buried channel waveguides by double ion exchange, the initial ion exchange must result in sufficiently large index change so that further processing does not decrease the index difference between the channel and substrate below a minimum acceptable value. For example, the maximum index change between Li-rich ion exchanged blass and Na-rich glass is approximately $\Delta n = 0.009$. Further processing such as thermal fusing or a second thermal ion exchange will decrease Δn well below satisfactory values.

Two factors make Ag^+ ion exchange a potentially favorable process for forming a buried waveguide. (1) A large Δn is obtainable, $\Delta n \sim 0.10$, (2) high index change can be drifted deeply into the substrate by applying an electric field during the ion exchange process. We have initiated experiments to form high Δn waveguides using an electric field.

Chartier et al.[1] has reported that evaporated Ag on glass can be drifted by an electric field into glass, replacing Na of the glass. We have performed initial experiments which appear to indicate that a thin surface waveguide layer has been obtained. However, we have had difficulty maintaining ionic current necessary for deep waveguide.

Fig. 2a illustrates the process and the masking of the glass substrate. The Al pattern is photolithographically formed on the glass substrate, as shown. A layer of Ag is then evaporated over the Al mask. A protective layer of Al is then laid over the Ag. An Al layer is evaporated on the reverse side of the glass substrate. An electric field (∿150 V/mm) is applied on the glass substrate, as shown. The glass temperature is increased to 250 to 300½C. Ag^+ ions then drift downwards replacing Na^+ of the glass. Na^+ ions then migrate downward to the glass-Al interface, forming a white layer.

The electric current through the substrate is indicated by an ammeter connected in series with the substrate. We have observed an increase of current to a peak of ∿4-10 ma as the substrate temperature is increased to ∿250-300°C. The temperature is maintained at ∿300°C. The current then falls in 5-10 minutes below 1 ma, then drops to a few μA as indicated in Fig. 3. The drop in current was unexpected and suggests that an electrical barrier to the electronic current has been formed by the migration, or, that the Ag ionic source has been depleted. (Calculations show that the latter does not hold). The electric current behavior has been observed during each of 5 times we have performed the experiment. External contact barrier between the gold wires and the Al layers has been

[1] G.H. Chartier, P. Jaussaud, A.D. deOliveira, and O. Parriaux, Electr. Lett. 14, 132 (1978).

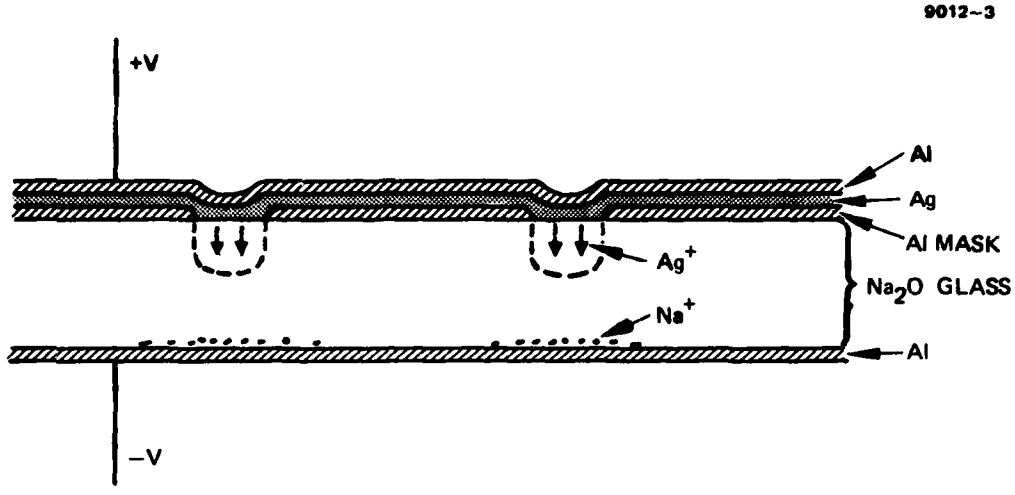

(a)

HRL MASKING CONFIGURATION

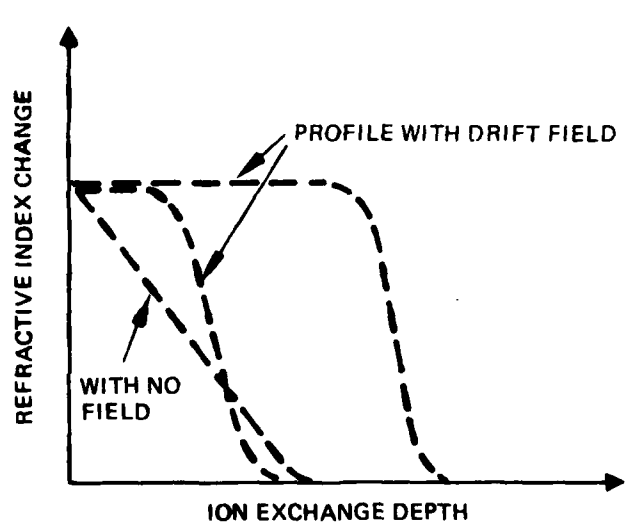

(b)

(AFTER CHARTIER)

Figure 2. Electric field assisted ion exchange experiment, where Ag replaces Na.
(a) HRL masking configuration
(b) Expected refractive index profile change (reported by Chartier et al.)

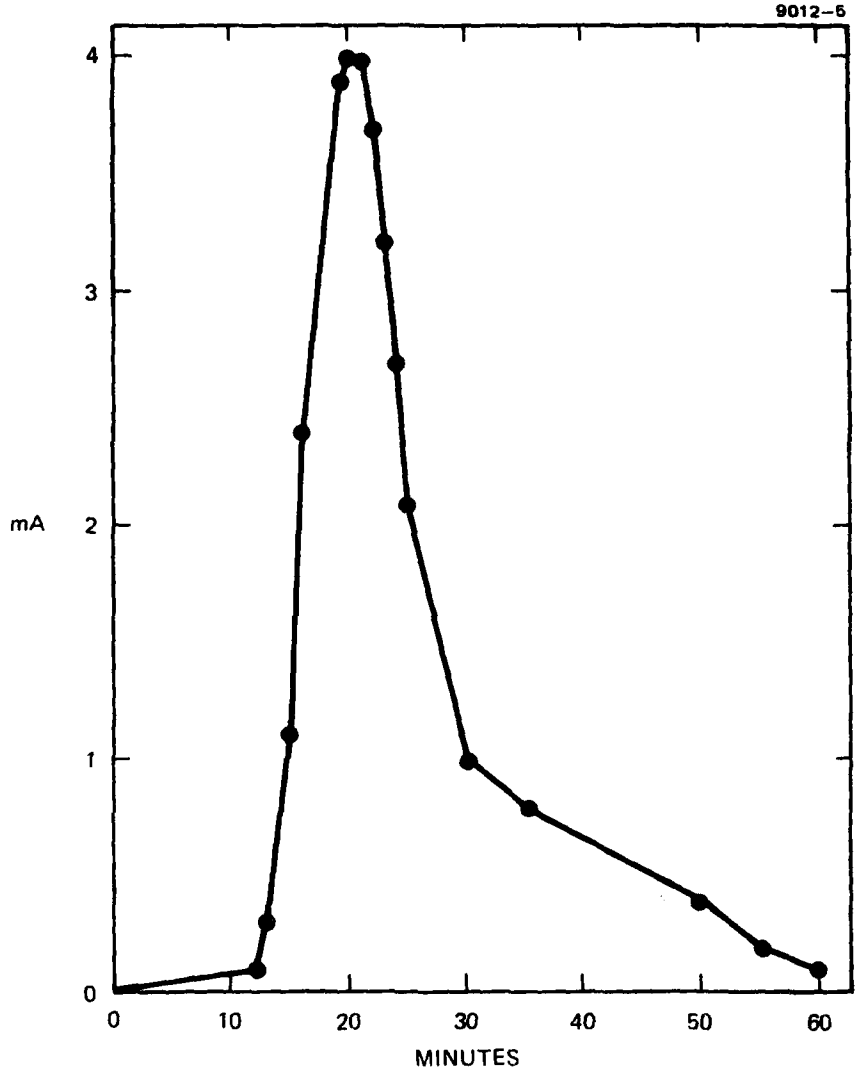

Figure 3. Current/time profile during electric-field assisted ion-exchange process.

ruled out since the very low contact resistance is measured on the Al surface after the experiments.

We might conclude that an electrical barrier has been formed at the glass to Al interface, arising from the migration of the Na^+ ions to that region. This study will be continued during the next period since the electric current attenuation forms a serious obstacle to the formation of deep waveguides by electric field assistance.

GLASS BUBBLES

We have found that ordinary plate glass and microscope slides contain minute bubbles which form scattering sites in ion-diffused waveguides. To correct this deficiency, thick slides of bubble-free Schott glass with 14% Na_2O was bought from a local vendor. Scatterfree waveguides were fabricated. Unfortunately, the waveguides were inferior to that fabricated from window glass. Subsequent investigation showed that the local vendor had provided us with 7.6 weight % Na_2O glass and not the 14% promised. We have since then ordered 14% Na_2O glass from another vendor.

SECTION 2

R&D PERIOD, 1 AUGUST 1978 TO 30 SEPTEMBER 1978

This report summarizes the work performed during the period from 1 August 1978 to 30 September 1978 on Contract F19628-78-C-0201 entitled "Fiber Optic Couplers". The report is divided into four sections. These are: 1) Theoretical Design of Fiber Optic Planar Couplers, 2) Material Processing for Planar Couplers, and 3) Plan for the Next Period, and 4) Program Schedule for this contract.

THEORETICAL DESIGN OF FIBER OPTIC PLANAR COUPLERS.

A ray-tracing investigation of the proposed multimode planar star and "Y" couplers was made in order to characterize the partitioning of light into the planar branches as a function of index profile, device dimensions and configuration. The losses of these devices were also tabulated. This study identified the important parameters of a planar design. For example, the required mixing length of a planar star coupler for equal partitioning of light into each of the channels was determinable by ray tracing. As another example, the channel widths and acute angle of a Y coupler were found to control the partitioning of radiation into the arms of the Y. The major portion of this ray tracing design investigation was performed under IR&D and is described here since the resulting designs will be fabricated under this contract. This section describes the ray initialization procedure, the tracking procedure and the data generated to date. It should be pointed out that straight line ray tracing requires that the planar guides and the substrate be uniform in refractive indices. The ray tracing analysis is limited to such planar structures. Whether the method is approximately valid for graded index planar guide needs further investigation.

In order to accurately simulate the devices, the rays must statistically simulate the total of the modes in the guides. Since the structure that is analyzed is a step index configuration, we have elected to choose the rays randomly such that the angular extent of the numerical aperture is filled uniformly. Although it is also possible to randomly choose the initial x, y position of the rays in some z plane, we elected to divide the input plane into a rectangular mesh and trace a single ray from the center of each rectangle. Using this algorithm and starting the random number generator

at different positions does not affect the final result significantly (>1% variation) if a large number (>5000) of rays are traced. That is, some average properties associated with the motion of a large number of identical systems differing over a range of initial conditions is obtained.

Given the initial values for position (x,y) and direction cosines (k, l, m) of a ray at some z_0(=0) it is possible, in general, to solve for its position and direction cosines at any other value of z. Although ray tracing is well understood the procedure is described.

Snell's law describes the refraction of light through an interface (Fig. 1) and is given by

$$n_2 \bar{S}_2 \times \bar{G} = n_1 \bar{S}_1 \times \bar{G} \tag{1}$$

or

$$(n_2\bar{S}_2 - n_1\bar{S}_1) \times \bar{G} = 0 \tag{2}$$

where

$\bar{S}_1$ is a unit vector in the direction of the ray impinging on the interface.

$\bar{G}$ is a unit vector in the direction of the local normal to the interface.

n_1 and n_2 are the refractive indices on the two sides of the interface.

$\bar{S}_2$ is a unit vector in the direction of the ray after refraction and/or reflection ($n_1 = n_2$) at the interface.

Equation (2) is a simple vector relation which can be solved exactly; it is satisfied if the vector in the parenthesis is colinear with $\bar{G}$, thus allowing one to write

$$n_2\bar{S}_2 - n_1\bar{S}_1 = \Gamma\bar{G} \tag{3}$$

or

$$n_2\bar{S}_2 = n_1\bar{S}_1 - \Gamma\bar{G} \tag{4}$$

where Γ is yet an unknown quantity. The dot product of Eq. (4) with itself eliminates the unknown $\bar{S}_2$ and gives the following quadratic equations in Γ:

$$\Gamma^2 - 2\Gamma(n_1\bar{S}_1 \cdot \bar{G}) + (n_1^2 - n_2^2) = 0 \qquad (5)$$

or

$$\Gamma = n_1\bar{S}_1 \cdot \bar{G}_1 \pm \sqrt{(n_1\bar{S}_1 \cdot \bar{G})^2 - n_1^2 + n_2^2} \; . \qquad (6)$$

By the appropriate choice of Γ, all situations that are encountered at a refractive interface can be accurately described. If the square root is imaginary ($n_1 \neq n_2$), the ray is totally internally reflected and the positive sign is chosen after setting $n_1 = n_2$

$$\bar{S}_2 = \bar{S}_1 - (2\bar{S}_1 \cdot \bar{G})\bar{G} \; . \qquad (7)$$

If the square root is real, the smaller absolute value of Γ will give the $\bar{S}_2$ corresponding to the physical situation of refraction (Fig. 1). Substitution of this value for Γ into Eq. (4) gives the new ray direction $\bar{S}_2$. In the analysis rays of this sort are lost from the device and thus summed to evaluate the losses.

The algorithm for ray tracing through a device is

a) initialize ray,
b) determine surface of intersection,
c) apply Eq. (7) if square root in Eq. (6) is imaginary. If square root is real, sum the ray as lost and go to (a),
d) repeat (b) and (c) until ray exits device,
e) sum ray as exiting appropriate port and go to (a).

Two structures have been analyzed to date; the planar star and Y coupler. The planar star configuration that has been analyzed is shown in Fig. 2. The inputs to the program are

θ = half angle of taper angle,
x_t = half width of wall,
x_B = half width of channel,
Y_B = half thickness of film,
z = mixing length,
Numerical aperture of the guide,
Index of the surrounding region,
Number of ports N.

Rays can be input at any of the ports, the program output is the number of rays that exit each of the ports and the number of rays that are lost. Figure 3 shows the results of varying the mixing length, Z, for an eight-port star coupler; each line represents the number of rays that exit a given port. The number of rays to each of the ports with ports 1 through 4 for input and z/x_B = 2750 are given in Table 1. The number of rays lost or not satisfying the condition for total internal reflection at any one of the guide wall intersections is also given in Table 1. A total of 10,000 rays were traced for each input.

TABLE 1.

Input port → Output port	1	2	3	4
1	1120	1030	1003	1030
2	1023	1018	1057	1035
3	1079	1050	1050	1144
4	1020	1111	1137	1090
5	1090	1110	1151	1107
6	1136	1135	1080	1169
7	1142	1117	1153	1080
8	1162	1177	1117	1093
Loss	1228	1252	1252	1252
Total	10,000	10,000	10,000	10,000

The planar Y coupler configuration is shown in Fig. 4. The inputs to the program are X_B, X, y_B, , the numerical aperture of the guide, the index of the surrounding region, and the input port. Using x as a parameter and θ as a variable, Fig. 5 shows the transmission properties

(port (1) to port (2)) of this device. Figure 6 shows the fractional transmission from port (3) to (1). Figure 7 shows the fractional transmission from port (2) to port (1). Further analysis will be performed to understand the variations in the low angle region of these plots.

The program has been expanded to determine the angular extent of the light coupled from one branch to the other; far field spot diagrams will be generated. The loss of coupling the square guide to a circular fiber will also be investigated. It is emphasized that all results presented in this section are calculated.

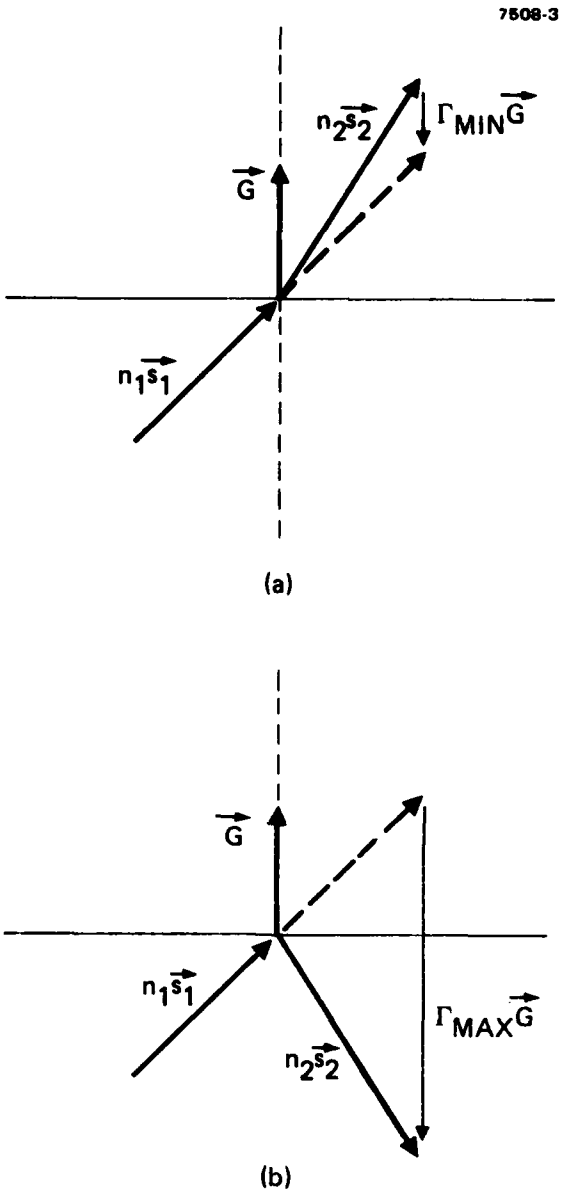

Figure 1. Illustration showing that the appropriate choice of Γ in the solution of Snell's Law is Γ_{min}.

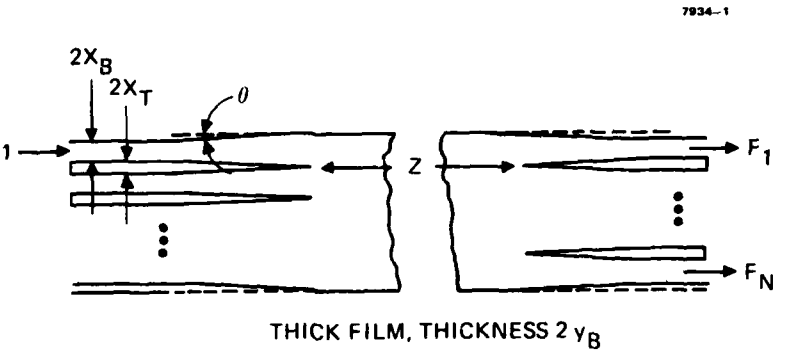

Figure 2. Schematic of a planar star coupler.

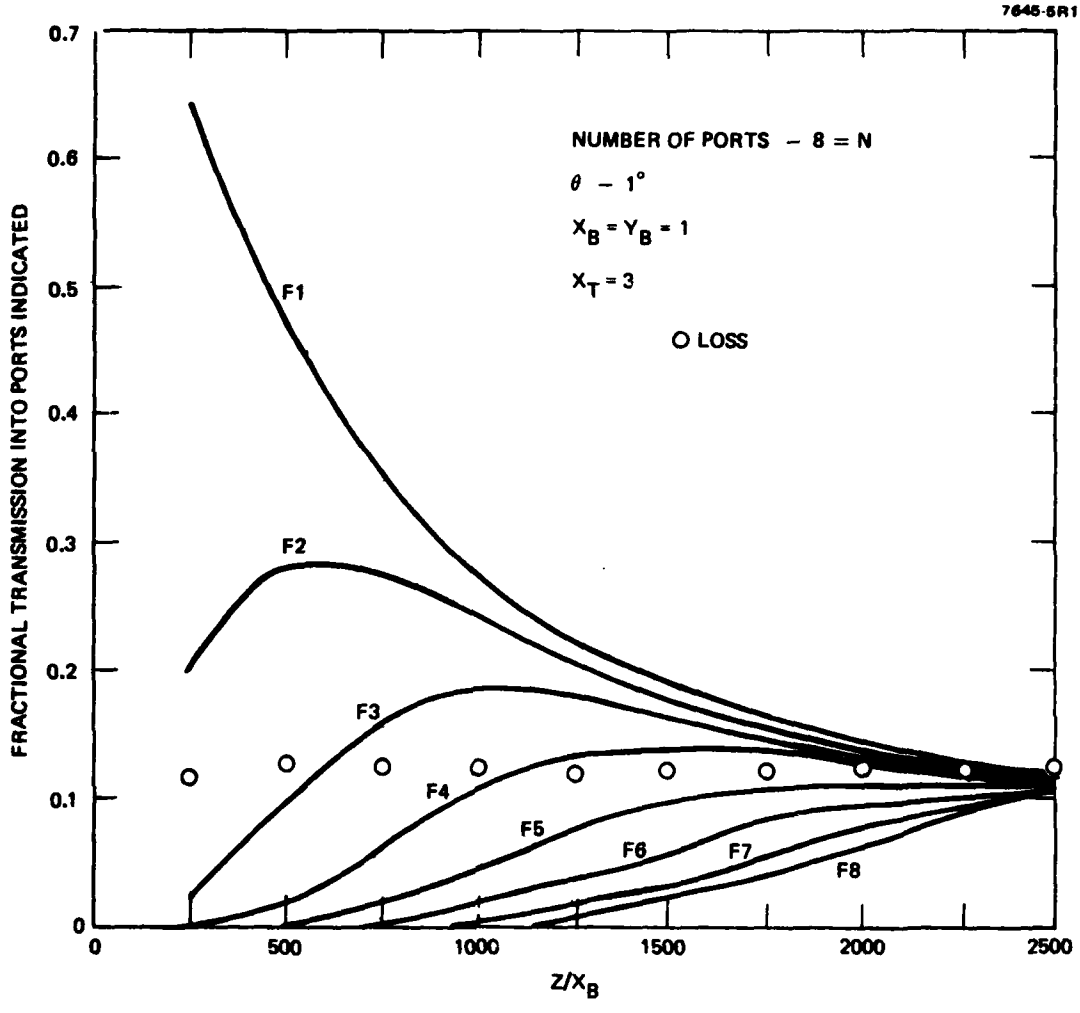

Figure 3. Fractional transmission of an eight-port planar star coupler versus the mixing length.

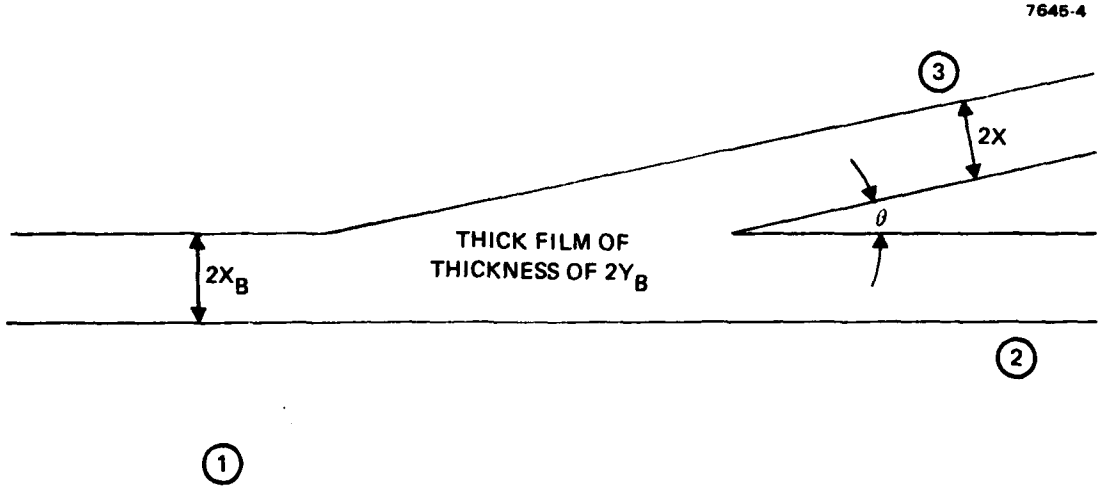

Figure 4. Schematic of the planar Y coupler.

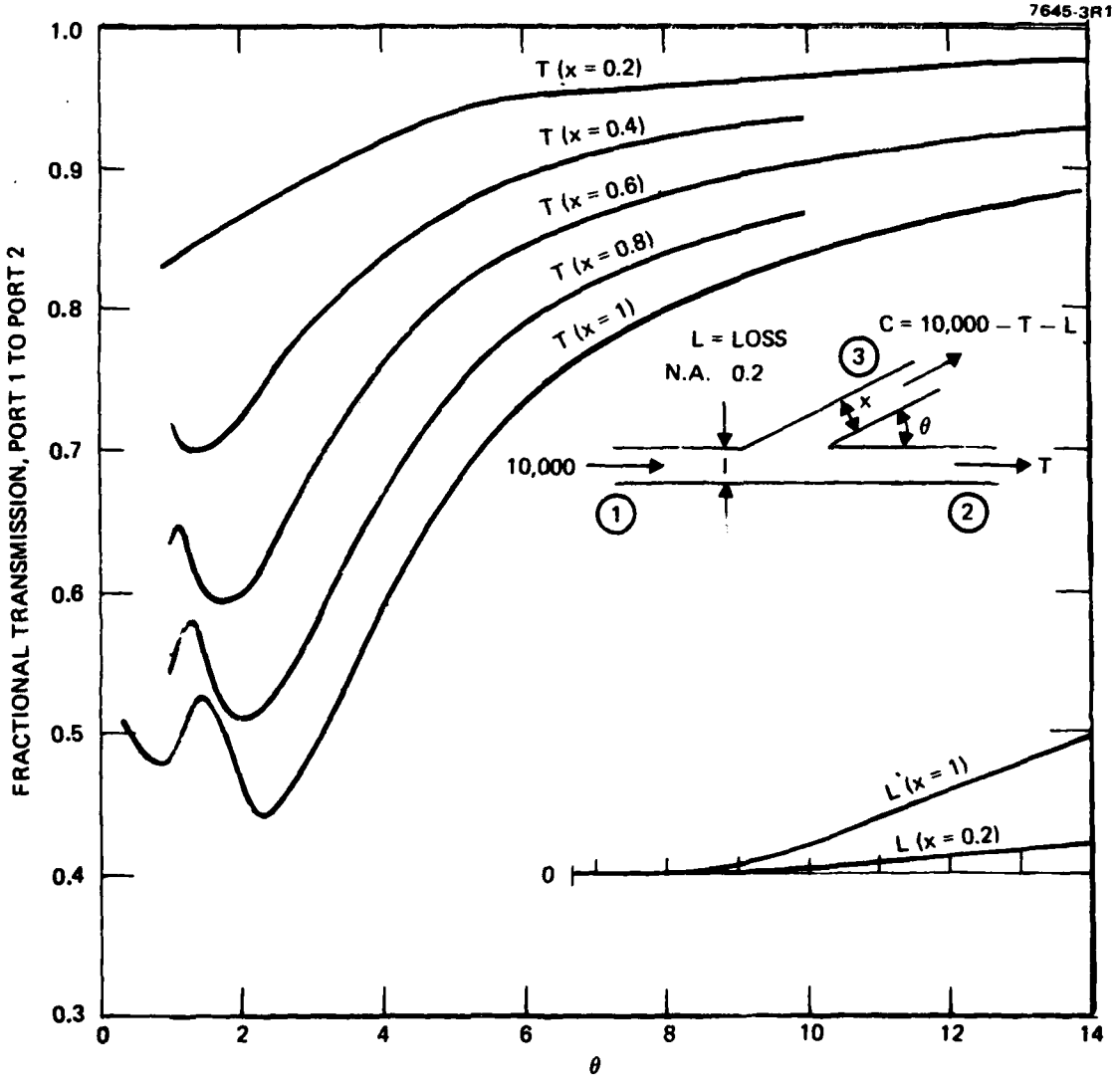

Figure 5. Fractional transmission from port 1 to 2 for the planar Y coupler versus the coupling angle. The fractional loss is shown in the insert; the width of the branch is used as a parameter.

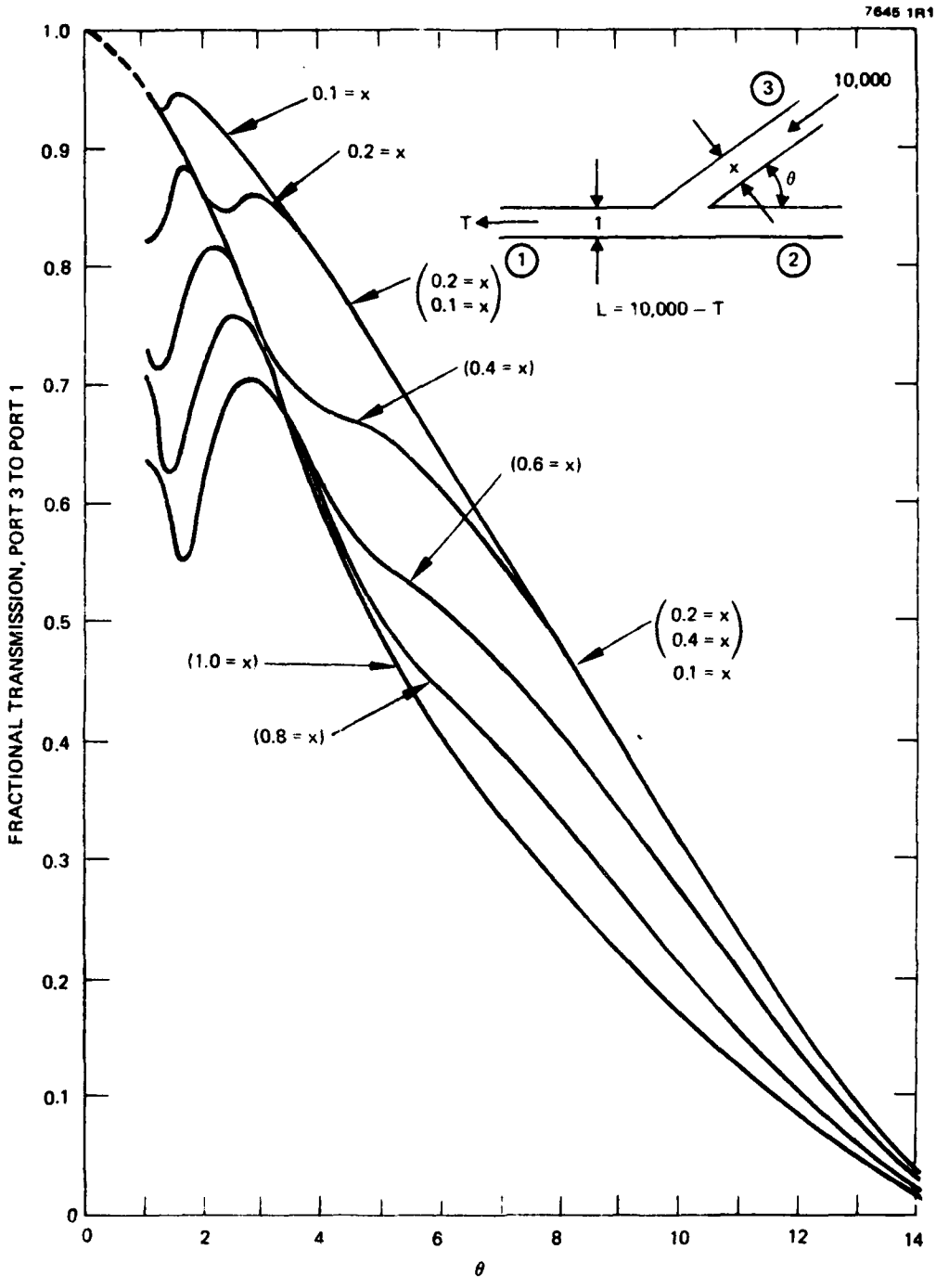

Figure 6. Fractional transmission from port 3 to 1 for the planar Y coupler versus the coupling angle. The width x of the branch is used as a parameter.

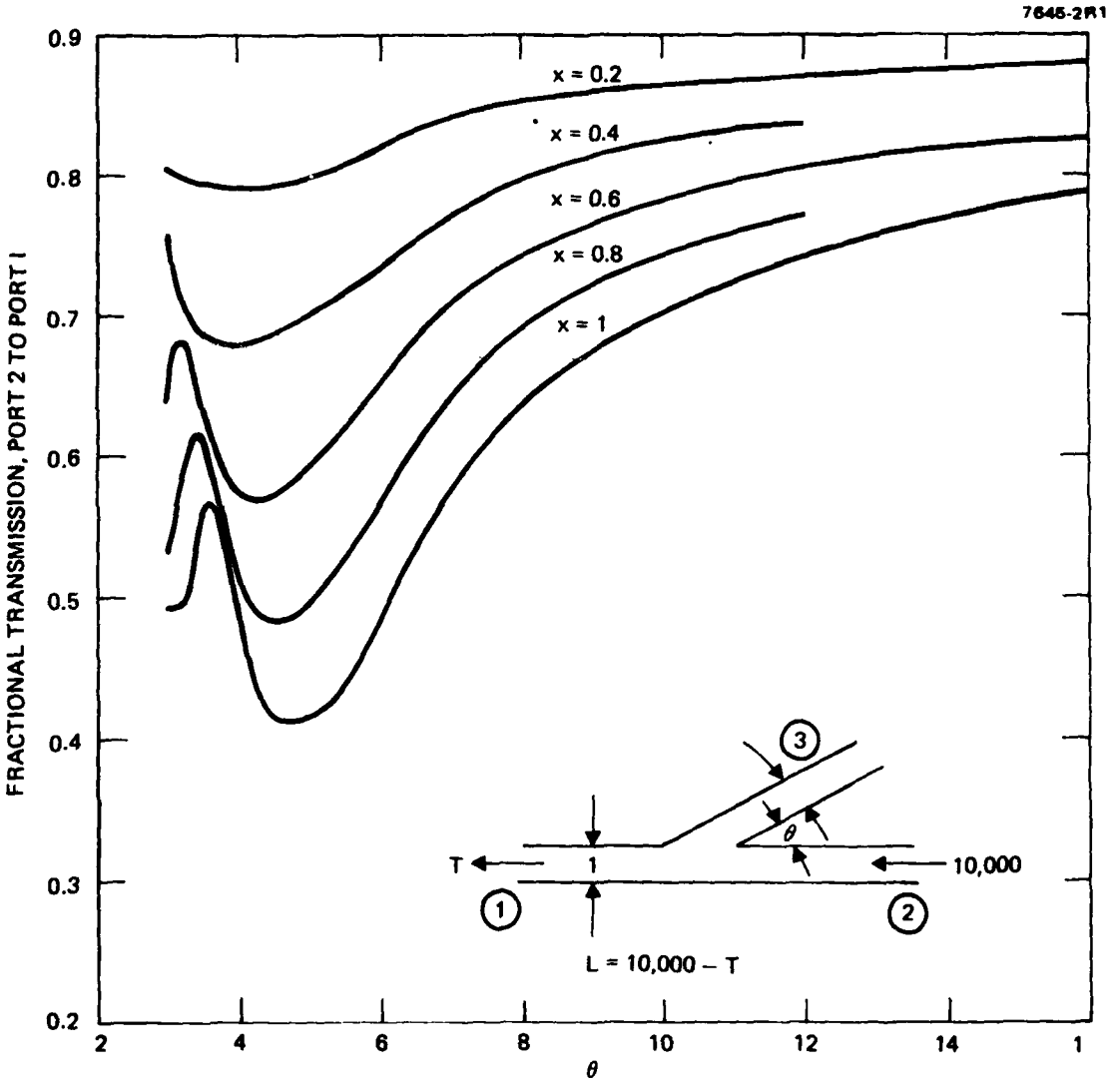

Figure 7. Fraction transmission from port 2 to 1 for the planar Y coupler versus the coupling angle. The width x of the branch is used as a parameter.

MATERIALS PROCESSING FOR PLANAR COUPLERS

Major developments in the area of material processing must be made during this program. We feel that the chief technical issues which must be addressed are the following:

- Optimization of the fiber-to-channel coupling; we have set as an objective a -0.5 dB coupling loss for both ion exchange systems.
- Processing reproducibility for the ion exchange must be thoroughly studied.
- Development of an SiO_2-based coupler system; this requires new planar processing techniques for deposition such as thick film CVD deposition or other techniques.

To carry out the tasks we have formed a materials processing team which will report to Dr. C. K. Asawa throughout the program. The team consists of researchers from both the Optical Physics Department (Dr. G. L. Tangonan and Dr. O. G. Ramer), and the Chemical Physics Department (Mr. A. C. Pastor, Dr. R. C. Pastor and Ms. L. E. Gorre). This contract program is directed by Dr. M. K. Barnoski. In the following discussion we deal with each of the technical issues listed above, with the emphasis being placed on material related issues.

Optimization of the Fiber-to-Channel Coupling

We have set as a reasonable goal the demonstration of -0.5 dB loss at the fiber-to-channel interface. This does not include the reflection losses and is ascribed to the mismatch of the fiber and channel guide optical mode characteristics. This is a key issue which we feel requires considerable attention since this coupling problem must be solved if planar couplers will ever be practicable. Our results on ion exchange planar waveguides already indicate that the planar approach is conceptually sound. High efficiency coupling still remains to be demonstrated.

The ion exchange channel guides which have been studied show an average coupling loss from Corning graded index fiber-to-channel guides of -1.9 dB. To measure this coupling a series of ion exchange experiments were performed

to form straight channel guides of varying mask openings (35, 45, 55, 65, 78, 85 μm). The ion exchange processing time was varied using 20, 25, 35 and 40 minutes. We found that the best parameters for coupling a graded index Corning film were for a 30-minute exchange with a 65-μm opening.

Our results indicate that careful control of the index profile is necessary to control the coupling. We are initiating the following steps to solve this problem.

- Investigation of a variety of melt systems which may be used to reintroduce the sodium ions taken out by the exchange process—this will lead to a buried guide structure which will better approximate the graded index of a fiber.
- Development of an index of refraction profiler which will measure the index profile in a simple and accurate way. To do this we will use a technique by Nippon Telephone and Telegraph (NTT) researchers which is based on the measurement of the reflection from the polished end-face.
- Theoretical estimates of the expected coupling losses for various profiles will be made. This will serve as a useful guide for the experiments and also serve as the basis for alignment tolerance studies.

Within the next two months a melt system will be selected and tested to perform the second exchange. We will then perform a series of exchange runs for channel guides and determine the effective coupling.

Processing Reproducibility for the Ion Exchange Process

At present we have not yet fully investigated the reproducibility of the process of guide formation. We feel that the process is controlled by several variables; variations in starting substrate glasses, aging of the melt due to decomposition, reactions of the melt with the glass slide, reactions with the metal mask. The variables must be controlled for highly reproducible device fabrication.

Variations in the starting substrate glasses which affect the Li-to-Na ion exchange are the composition differences between slides, surface condition such as the presence of microcracks, scratches, etc., and the differences in thermal history and stress history. At present we are assessing the relative importance of these parameters and the degree to which they

affect the index profiles of the resulting guides as well as the geometrical integrity of the slides after processing (bowing effects or flatness deviations).

The role of chemical reactions between the melt with the glass slide and the melt with the melt mask may cause variations which affect the processing. These parameters are under investigation. We have found a slight thinning of the sample occurs during the ion exchange. This seems to be a major reaction. The reaction chemistry will be investigated in the next two months and a detailed report will be given then.

SiO_2-based Planar Couplers

The major emphasis in the materials program is being placed on development of planar couplers on SiO_2. Our approach is that summarized in the following schematic diagrams of the fabrication process. The objective is to form a well-defined pattern of a waveguide structure which closely simulates a conventional fiber (graded index). To do this, a first step is to deposit a ≈10-μm thick layer of a dopant glass layer (Fig. 8). This glass layer could be of a variety of oxide glasses (or mixture of glasses) with the high index of refraction, such as GeO_2 and $Li_2O \cdot Na_2O \cdot SiO_2$ glasses. The deposition may be carried out using two techniques—chemical vapor deposition (CVD) and dip melting. Both of the processes have been attempted at HRL with good indications warranting further study. These techniques are discussed later. Conventional photolithographic processing is then used to form a dopant pattern, say, in the shape of an asymmetric Y branch. As a result of this step, the process derives the advantages of versatility, reproducibility and batch processing commonly achieved with planar processing. The dopant pattern is then overcoated with a thick layer of SiO_2 (≈100 μm thick). This thick layer and the SiO_2 substrate thus completely surround the dopant pattern. A high temperature, thermal diffusion process is then incorporated. The diffusion of the dopant into both the overlayer and the substrate is expected to result in a graded composition and therefore a graded index of refraction. By controlling the diffusion process, guide patterns which closely simulate conventional fibers may be made using planar processing.

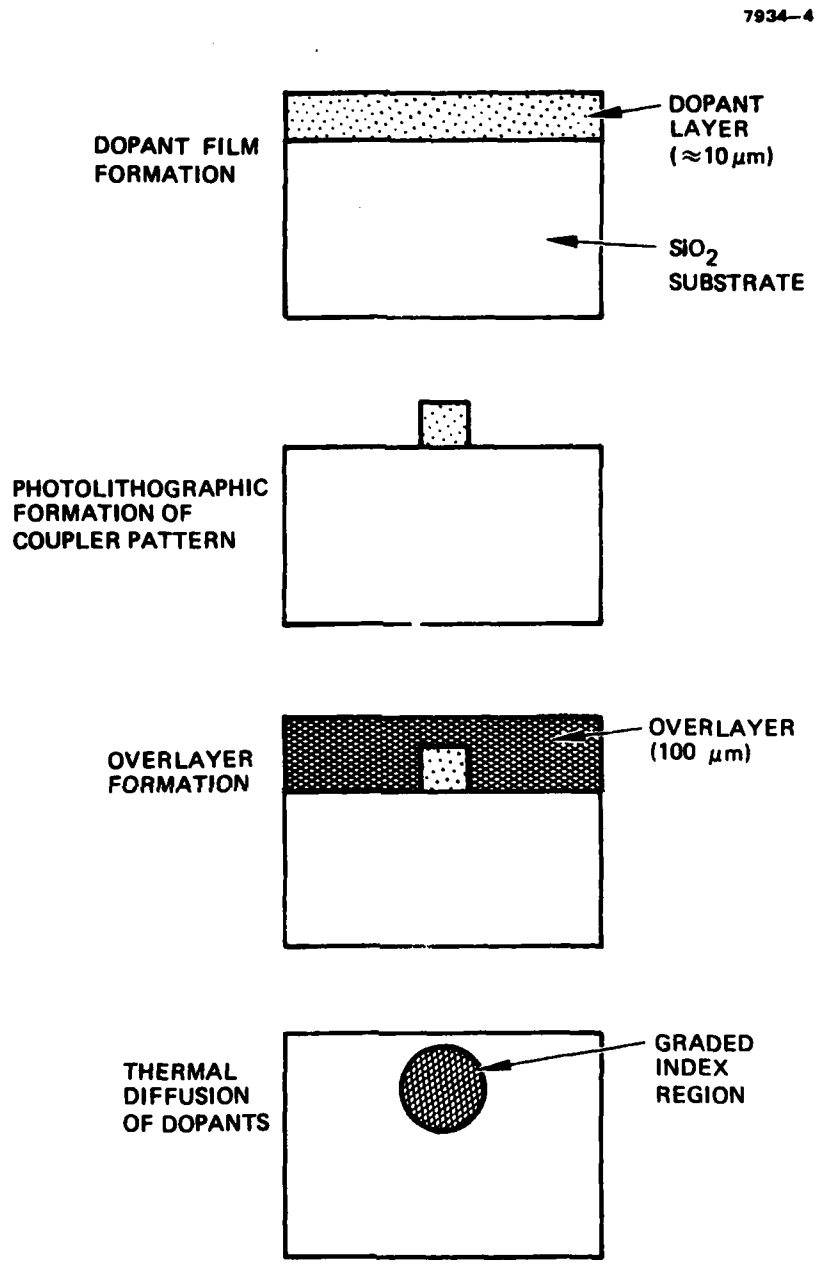

Figure 8. SiO_2-based planar coupler.

The key technical issues involved in developing this multi-step process are summarized in the following questions:

- Can suitable dopant layers be deposited on SiO_2 substrates with 10 μm thickness and good optical quality? This process must be fairly rapid and should not rely on conventional evaporation or sputtering approaches.
- Can the overlayers of SiO_2 be deposited with rapid deposition (1 μm/minute, for example) and with good optical quality? Can this be done with a process which preserves the dopant pattern defined by the photolithographic step?
- Can the controlled diffusion of dopants be achieved to form guide structures with ≈60 μm guiding cross-sections for the 10 μm x 10 μm dopant source cross-sections?

To answer these questions, we have initiated a materials program aimed at solving each of these problems. The two techniques we have investigated in detail are CVD, using metalo-organics, and the dip-coating process. These two techniques are summarized in the following sections.

Metalo-organic CVD Process. We have demonstrated that metalo-organic compounds may be reacted to form thick oxide deposits >20 μm in a short time period of ≈30 min. These experiments were performed last year under IR&D funding for planar couplers. The chemical reactions involved in depositing, for instance, glass mixtures of SiO_2 and GeO_2 are

$$(C_2H_5O)_4\ Si + 12\ O_2 = SiO_2 + 8\ CO_2 + 10\ H_2O$$

$$(C_2H_5O)_4\ Ge + 12\ O_2 = GeO_2 + 8\ CO_2 + 10\ H_2O.$$

These reactions are localized onto the SiO_2 substrate surface, as shown in Fig. 9 by

1) heating the substrate to a temperature high enough to ignite the jet of reactant gases impinging on it,
2) diluting the combustible alcoholate vapors with an inert carrier gas (nitrogen), to prevent backward flame propagation along the gas jet. Molar volume composition which we have used is O_2:N_2:alcoholate vapor: 18:18:1.

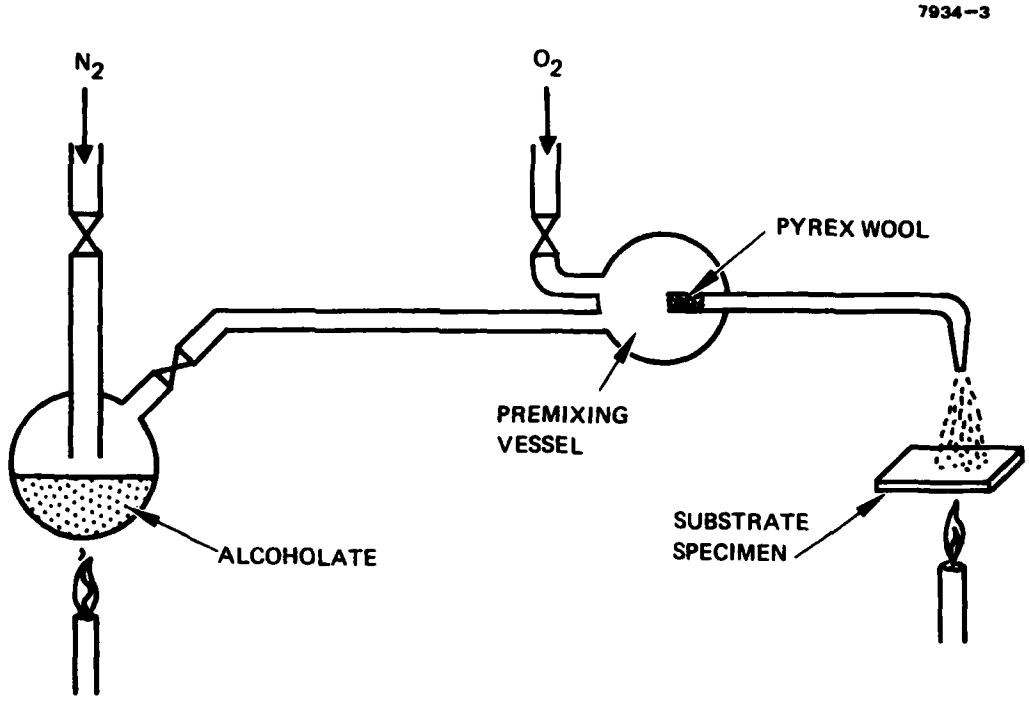

Figure 9. Metallo-organic CVD process.

In conventional CVD for silicon technology, the combustion of silane (SiH_4) and germane (GeH_4) would be used for this purpose. For our case, however, the silane burns too rapidly and therefore its combustion reaction is extremely difficult to localize. The localization allows rapid thickness buildup in our process. This situation is just as bad for germane as well as any other method involving the hydrolysis of the tetrachloride species.

In the following months we will construct a new reactor for the CVD process. Our first experiments were halted because of an explosion which occurred due to uncontrolled backward flame propagation. The new system under construction incorporates adequate measures which will control the back streaming.

During the next period we will examine briefly CVD surfaces formed by conventional processes used for forming optical fiber. A two-inch diameter SiO_2 tubing, with CVD layer on the inner surface, will be diced into small segments. We will examine the potential for photolithographic processing of waveguide channels on the curved surfaces and the optical scattering resulting in the CVD layer. The effort will be minimal, since an ongoing project for fabricating optical fiber preforms exists at Hughes Research Laboratories.

Dip-Coating of Glasses

A technique which we have demonstrated which is readily applied to the deposition of the first layer—the dopant layer—is dip-coating. This technique is very simple. We have demonstrated that thick films ($\sim$10 μm) of PbO-B_2O_3-SiO_2 glass can be deposited by this method. This technique involves melting the glass material in a Pt crucible and introducing the substrate material into the melt. By controlling the temperature, the glass viscosity, and the pulling rate, glass layers of differing thickness can be deposited. To prevent cracking of the composite due to differential contraction (upon cooling) the layer is allowed to diffuse into the substrate. A graded composition structure occurs which prevents cracking in most systems. This process is shown in Fig. 10.

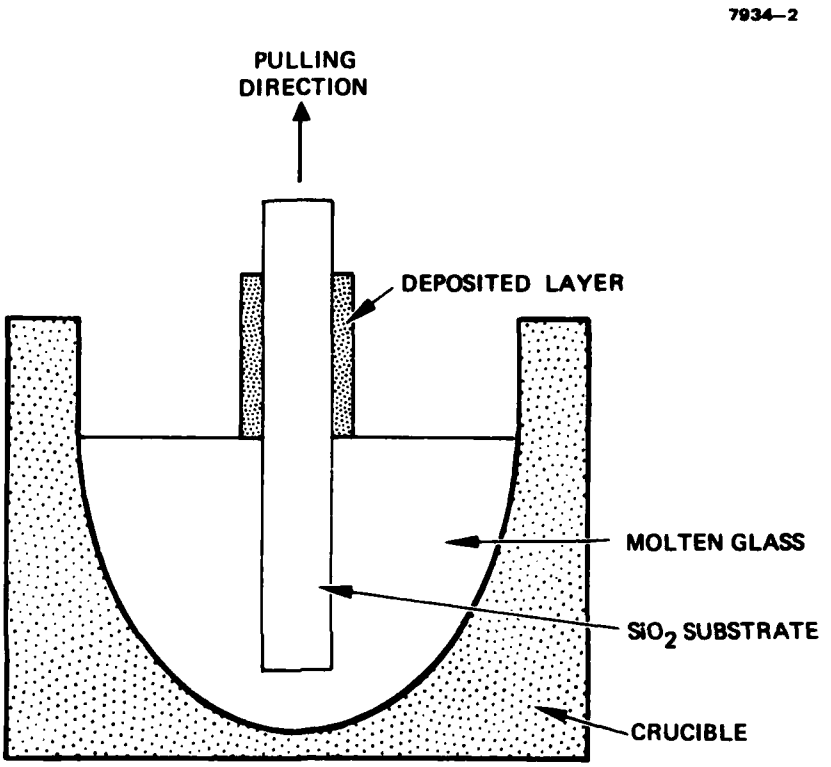

Figure 10. Dip coating of glasses.

During the next two months we expect to demonstrate 20 μm thick layer deposition of a variety of glass layers such as $PbO-B_2O_3-SiO_2$ and $Na_2-B_2O_3-SiO_2$, $GaO_2-B_2O_5-SiO_2$ with this technique. A determination of the diffusion rates of the dopant layer into the SiO_2 substrate can then be conducted. We anticipated the diffusion rates will be strongly determined by the valence of the diffusant. Dopants with low valence (Li^+, Na^+, B^+) will diffuse more rapidly than Ge^{4+}, for instance. The studies will lead to valuable information about the final diffusion step.

SECTION 3

R&D PERIOD, 1 OCTOBER 1978 TO 30 NOVEMBER 1978

This report summarizes the work performed during the period from 1 October 1978 to 30 November 1978 on Contract F19628-78-C-0201 entitled "Fiber Optic Couplers". The report is divided into four sections. These are: 1) Theoretical Design Analysis, 2) Optical Measurements on Planar Devices, 3) Planar Coupler Processing, and 4) Plan for Next Period.

THEORETICAL DESIGN ANALYSIS

The ray analysis of the planar Y coupler has been expanded in order to describe coupling of cylindrical fibers to planar guides with square cross-sections. The analyses previously reported were for a Y coupler shown in Figure 1a, with the input and output spanning the indicated square cross-section of the planar guide. During this period two modifications shown in Figure 1b were made in the ray tracing computer program: (1) An extra bend was incorporated in the upper branch to render it parallel to the lower branch (for the purpose of simplifying fabrication), (2) Rays enter the planar guide of square cross section from a cylindrical fiber core, where the core diameter equals the length of the sides of the square; the rays exit the planar guide into a similar fiber core.

For the geometry of Figure 1b, the fractional transmission into the exit fiber as a function of the acute angle θ of the coupler are shown in Figure 1c. 7860 rays were used in the computer program. The fibers and ports of the planar couplers are indicated by 1, 2 and 3. The fractional transmission from fiber i to fiber j is indicated by T_{ij}, where i,j = 1, 2, and 3. As examples, T_{13} is the fraction of rays transmitted from fiber 1 to fiber 3, T_{31} is the fraction from fiber 3 to fiber 1. T_{32} and T_{23}, being small for the indicated angles, are not shown.

With input at 1, the excess loss due to the additional bend at B is increased with bend angle $\theta > 4°$, with a maximum of 0.11 at 7.5°. At larger angles the bend loss decreases since coupling to the upper branch decreases. The total loss shown in Figure 1c includes the bend loss and also includes the loss of $\sim$0.2 at low angles arising from area mismatch at the exit port.

The results of these calculations again show that branching ratios can be specified by the magnitude of the acute angle θ. For example, if a branching ratio (T_{12}/T_{13}) of 3.6 is desired, θ is determined to be 5.5°.

During the next period we will determine the feasibility of modifying the program ray tracing to account for the graded index profiles. Rays will be tracked through a multilayered structure of differing refractive indices. This effort will be small.

OPTICAL MEASUREMENTS OF PLANAR DEVICES

We have fabricated fourteen (14) planar reflection stars, six (6) transmission stars, twenty (20) new sets of uniform width planar channels, two (2) fiber ribbon connectors, and three (3) etched silicon fiber-alignment guides. Thin sections of planar guides were also prepared for refractive index profile measurements. Buried planar guide on microscope slide has been fabricated by a two-step ion exchange process. These devices and the status of the process or optical measurements of these devices are summarized in Table I.

Eight-port reflection star couplers were fabricated by a process described previously. Aluminum films were evaporated on microscope glass slides, then photoetched with open area corresponding to the planar star design. The slide was then dipped in a molten solution of Li_2SO_4-K_2SO_4 at 580°C for twenty (20) minutes to ion-exchange Na of the glass with Li of the melt. The slides were then sawed, ground and polished. Silver mirrors were then evaporated on the reflection ends of the stars. The result was the first batch of eight-port reflection star couplers on microscope slides.

Optical properties of the reflection star couplers were then determined. By using two bent fibers, we were able to input light into any channel with one of the fibers and then extract the output of any of the other channels with another bent fiber. (The fibers were bent with a torch.) Our measurements of the total transmission of any seven (7) channels of star couplers referenced to input into the other channel was approximately -13 dB. We believe that the main sources of the loss for the initial batch were surface scattering arising from surface imperfections (the surface was not processed prior to ion exchange), mismatch of the refractive index profiles of the fiber to the planar channels, losses at the horns, and possible rounding of the mirror surface during polishing. Subsequent measurements also indicate that the effective NA of the planar channel is small compared to that for the graded index fiber. The result is inefficient coupling of the Corning graded index input fiber (NA at launch, .32 - .14) to the planar channel. Inefficient input coupling occurs since the higher order modes of the fibers are not coupled into the low NA planar channels. We also noted that the coupling depends critically on the relative profile positions.

Table 1. Fabricated Devices and Status - 30 November 1978

Fabricated Devices	Status
A. 8-Port Reflection Star Couplers.	Initial fabrication. Low NA.
On microscope slides (9 devices)	Microscope slides bent. Considerable scatter, throughput 13 dB (with fibers)
On polished window glass (6)	Almost no surface scattering with polished window glass. Improved performance, throughput - 11 dB. Optical measurements incomplete.
B. 8-port Transmission Star Couplers	4-1/2 inches long. Possible incomplete formation of horns and channels.
On unpolished window glass (6)	Ion exchange for upper volume of melt during processing appears to be poor. Quantitative optical measurements to be made.
C. Constant Width Channels	Two sets: old set fabricated several months ago.
20 old sets, 10 channels per set	Channel width 25, 40, 50, 65, 80, 90, 250, 325, 500, 620 μm.
20 new sets, 10 channels per set	Extensive optical measurements on old set.
	New set not examined optically.
D. Fiber Ribbon Connectors (2)	Fabricated with fiber spacer. Problem: dimensional mismatch with star coupler channels (mask dimension smaller than specified). Fabrication procedure discontinued.
E. Etched Silicon Alignment Channels (3)	To be used for aligning multiple fiber ribbon (for mating to star coupler). Forms excellent fiber alignment guides.
F. Reflection Stars with Different Processing Times	To determine effect of different ion exchange on refractive index profile. Optical measurements to be made.
20 min (14) includes A, above	
15 min (3)	
10 min (3)	
G. Buried Planar Guide with Two Step Ion Exchange Process	Evidence of layer burial not yet observed. Li ion exchange overlaid with Na ion exchange. Further optical evaluation to be performed.
H. Thin Sections of Planar Guides for Refractive Index Measurements	Optically examined with interference microscope. $\Delta n = 0.0086$. Detailed refractive index profile not completed.
I. CVD Guide in Cylindrical SiO_2 Tube	GeO_2, B_2O_3, SiO_2, P_2O_5 layer 100 μm thick on SiO_2. Optical fabrication results in shattering, or crazing, of layer.

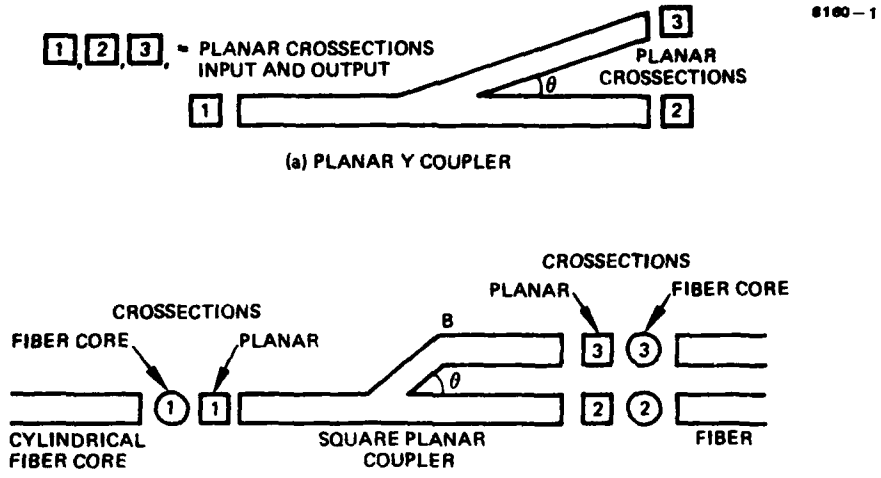

Figure 1. Theoretical design analysis of planar.

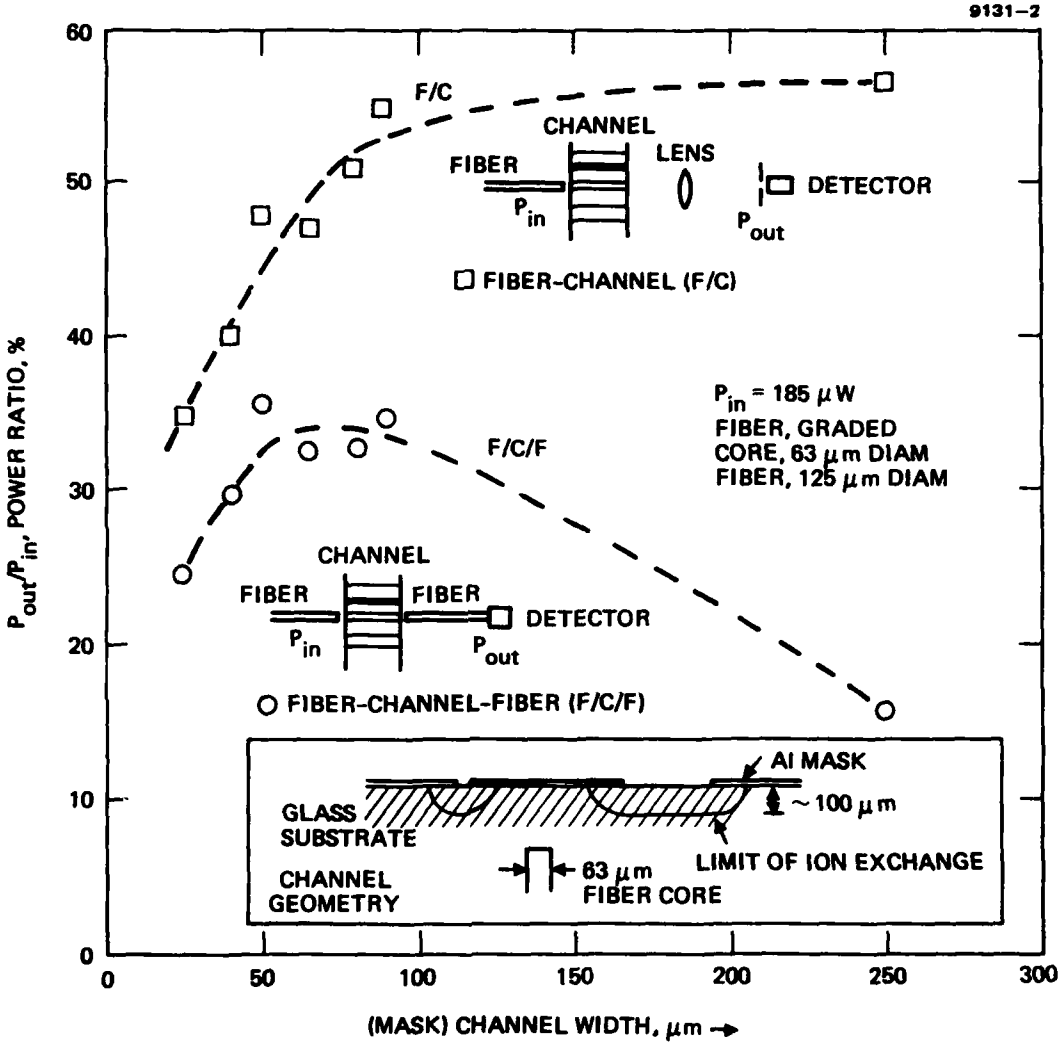

Figure 2. Power transmission ratios of constant width channel versus channel widths for fiber-to-channel coupling (F/C) and fiber-to-channel-to-fiber coupling (F/C/F).

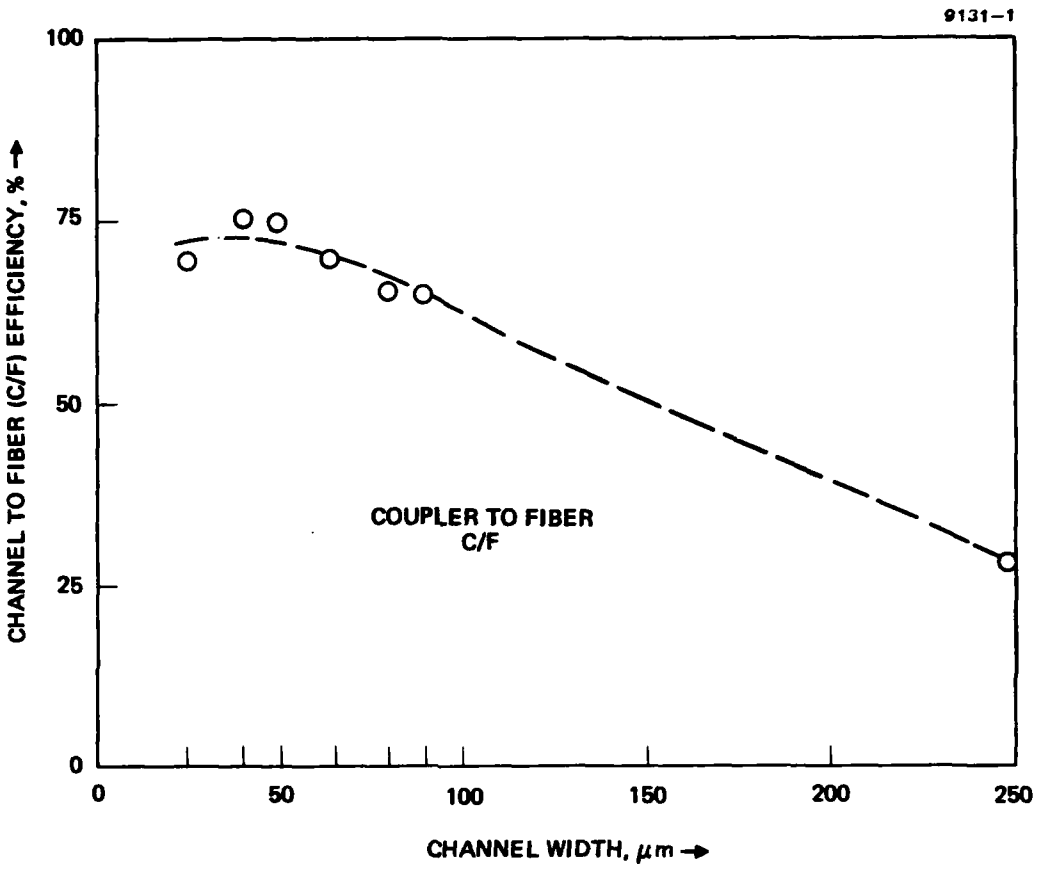

Figure 3. Channel-to-fiber coupling efficiency versus channel widths.

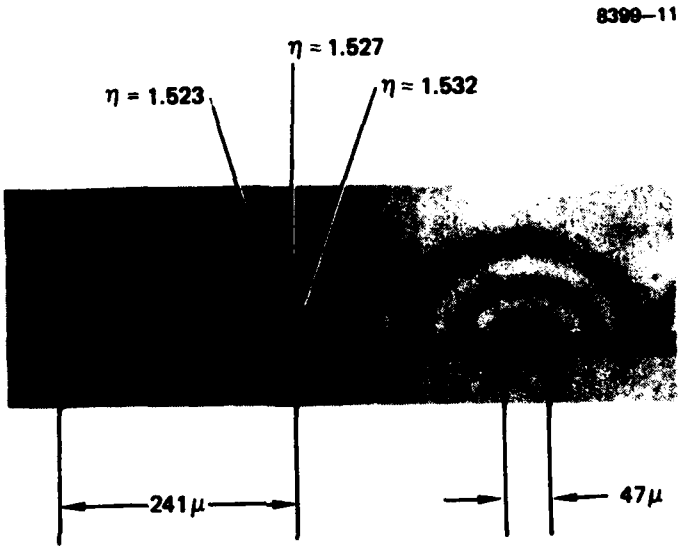

Figure 4. Interference microscope photograph of a star coupler cross section showing change of index of refraction. Center-to-center channel spacing and mask opening width are shown along with the indices of the substrate and ion exchanged channels.

The reflection stars fabricated in polished window glass showed very little surface scattering. Preliminary throughput measurements indicate an improvement of 1 to 2 dB over the unpolished microscope slides. Complete evaluation of these couplers will be made in the next period.

In order to determine the optimum width of a constant width channel for best fiber-to-channel-to-fiber coupling, a series of measurements were made on existing slides of straight channels of varying widths. Channel widths (of the mask) of 25, 40, 50, 65, 80, 90, 250, 325, 500, and 620 μm and channel lengths of one inch were available on previously fabricated slides. The slides had been dipped into the melt for twenty (20) minutes. The ion exchanged regions for various channel widths of the mask are shown schematically in the inset of Fig. 2. The diffusion of Li ions underneath the masks is indicated. The diffusion depth (∿100 μm) is determined by length of dipping (20 minutes) and melt temperature (580°C). Graded index fibers of 63 μm core and 125 μm o.d. were butt coupled to each end of a channel. Our measurements indicated that maximum throughput for fiber to channel to fiber (∿ 35%) occurred over a broad range of widths, 45-80 μm, shown in Fig. 2 and indicated by F/C/F. The fiber-to-channel output versus channel widths are indicated by F/C in Fig. 2; the near field is focussed on a detector with a lens, with an iris to isolate the channel throughput from scattered light. The efficiency of coupling from the output channel to the fiber can then be estimated by taking the ratio of (F/C/F) to (F/C); the ratio is shown in Fig. 3 as a function of channel width, with a maximum of ∿75%.

The refractive index profile of the ion-exchanged channel was examined. An interference microscope photograph of a thin section of three channels is shown in Figure 4 . The highest index is 1.532, the region that directly contacted the melt, and the lowest is 1.523, that of the glass substrate. For a step index profile, these indices would correspond to an NA = .16; however, the NA for the actual graded channel depends precisely upon the profile shape and launching conditions. The refractive index profile shape will be measured precisely during the next period.

Figure 4 clearly illustrates that ion exchange occurs under the Al-masked area, diffusing laterally as well as normally into the glass. The diffusion distance normal to the surface is ∿100 μm. Smaller mask openings would result in a more circular refractive index pattern.

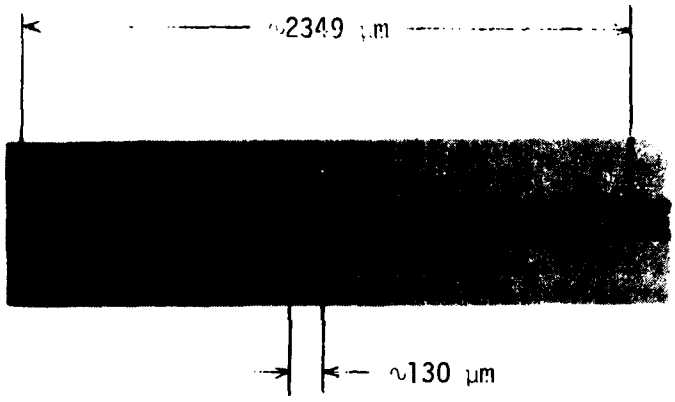

Figure 5a. End view of fiber ribbon connector.

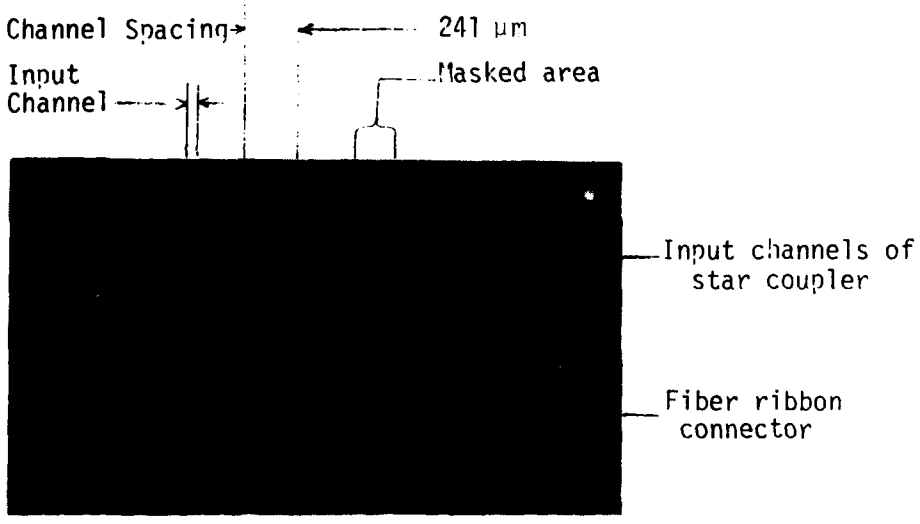

Figure 5b. Photograph of the input end of a star coupler with mating fiber ribbon connector. Note alignment mismatch.

PLANAR COUPLER PROCESSING

Since the Li_2SO_4-K_2SO_4 melt gave us problems of decomposition to the oxide and reaction with Al mask, the possibility of using an LiCl-KCl melt was considered. The same molar ratio (80% LiCl - 20% KCl) was used at the same processing temperature (580°C) under an He/CCl_4 atmosphere (Fig. 6). After a 30-minute equilibration above the melt, a microscope slide was dipped in the melt for twenty (20) minutes. A network of "fibers" formed on the surface of the slide, appearing as elongated bubbles under the microscope. Based on the results of the preceding experiment, it was concluded that this network was made up of microcracks. These were preferentially attacked by the melt, having higher localized free energy. The next slide was pretreated with 5% HF for five (5) minutes, then equilibrated and dipped in the melt. This procedure drastically lessened the density of the microcracks; however, it did not completely eliminate them. A third slide with an Al mask was dipped into the solution. However, the Al mask was attacked, decomposing according to the equation

$$Al + 3Cl \rightarrow AlCl_3 .$$

This corrosion can very likely be avoided by shifting to an He atmosphere after cleaning up the chloride melt in the He/CCl_4 atmosphere for a period.

The problem of microcracks also exists in the Li_2SO_4-K_2SO_4 melt, although to a lesser extent because of the solvent action by the oxide from the decomposition of the sulfate. Here, instead of a fibrous network, the high free energy areas form "pits." Thus, regardless of the nature of the melt used for ion exchange, the more basic problem seems to be obtaining crack-free slides as the substrate.

After studying the phase equilibrium of the $LiNO_3$-KNO_3 mixtures, we concluded that such a mixture was not suitable for ion exchange because of its low operating temperature constraint (530°C). We need a processing temperature of 500-550°C, but decomposition to the oxide takes place at these temperatures.

For the double exchange, a melt of 100% $NaNO_3$ was prepared. Slides which were previously dipped in the Li_2SO_4-K_2SO_4 melt were dipped in the $NaNO_3$ melt at 450°C/2h, 500°C/2h and 500°C/16h. Optical evaluation of first two slides was attempted using fiber guided optical excitation of the planar guide. It was difficult to observe the extent of the index of

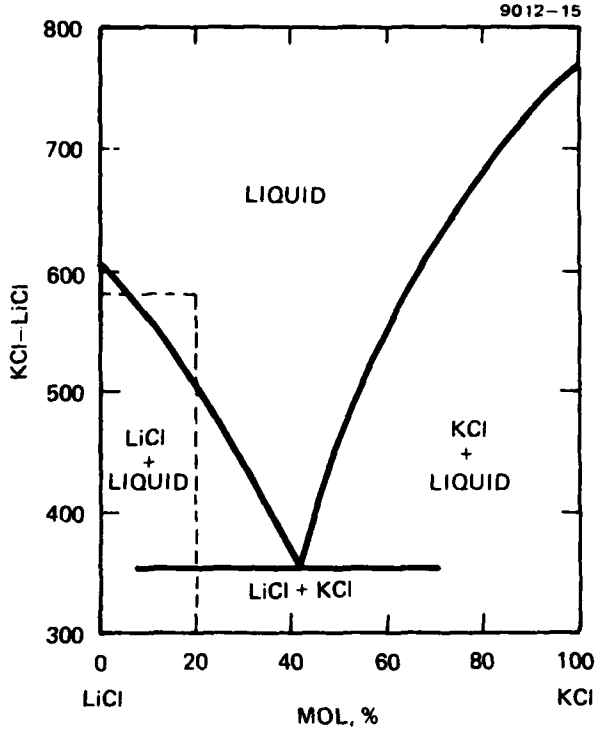

Figure 6. Phase diagram of the LiCl-KCl system. The dashed line indicates the operation points for the ion exchange formation. (From E. Elchardus and P. Laffitte, Bul. soc. chim., France, 51, 1572 (1932). See also S. Zhemchuzhnui and F. Ramback, Z. anorg. Chem. 65, 406 (1910.)

The refractive index profile of constant width channels also will be measured and correlated with the far field transmission pattern of the channel during the next period.

Two ribbons of eighteen (18) fibers (including fibers as spacers) to mate with the 8-channel star were fabricated. The cross section of one of the ribbons is shown in Figure 5a. Assuming that the fiber diameters were constant at 125 μm, an 8-port star mask was specified with interchannel spacing of 250 μm. Figure 5b illustrates dimensional mismatch arising from variations in fiber diameter and improper mask dimensions; the fiber spacings are greater than the channel spacings. The above fabrication procedure has been discontinued. Etched silicon alignment grooves (developed by BTL) will now be used to fabricate the fiber ribbon. Preliminary etching experiments have been performed and clean V-grooves in silicon for the fibers have been fabricated. The silicon groove method will be described further in the next report.

In summary, the results and conclusions of the optical measurements are

1) The maximum channel refractive index difference was $\Delta n = 0.0086$. Δn should be increased in order to match the fiber profile more closely.
2) Fiber-to-channel-to-fiber throughputs were measured to have a broad maxima of ∿35% for channel widths of 45 to 80 μm for the fabricated channels. This result includes channel scattering losses and channel-to-fiber coupling losses resulting from refractive index profile mismatch at both the input and output. The graded index fiber has core diameter of 63 μm, o.d. of 130 μm, and an input NA of .34 to .14. Closer matching of profiles are desired, such as with buried channels; increasing channel refractive index relative to that of substrate is desirable even with present structures.
3) The output channel-to-fiber losses for channel widths of 45 to 80 μm are ∿ 25%.
4) From the straight channel experiments, we can estimate that the power entering a star coupler is > 57% with present processing. We expect that a well fabricated star coupler will have total throughput somewhat greater than the above value.

refraction reduction at the surface (or channel burying). This process will be examined further during the next period. The possibility of using a mixture of $NaNO_3$-Na_2SO_4 (Fig. 7) will be examined further.

By conventional CVD process for forming fiber preforms, we fabricated 100 μm deep channel waveguide layer composed of GeO_2, B_2O_3, SiO_2, P_2O_5, on the inner surface of a 10-cm diameter SiO_2 tubing. The waveguide layer unfortunately crazed during several attempts to cut the tubing. During the next period another trial will be made using a different proportion of the above ingredients in order to try to alleviate built-in stresses in the layer.

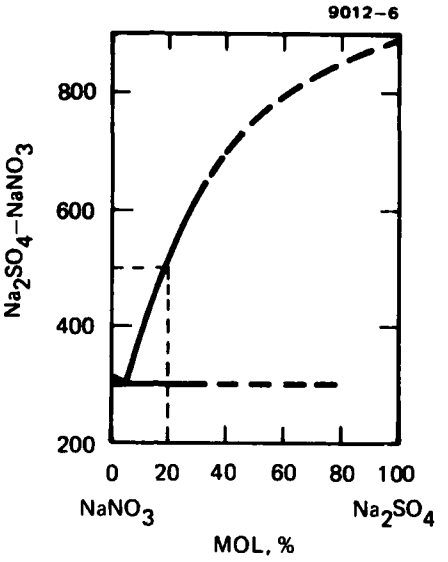

Figure 7.
Phase diagram of the $NaNO_3$-Na_2SO_4 system exchange conditions at the dotted line will be our operating point. (From M. Amadori, Atti reale accad. Lincei, Sez. II, 22, 334 (1913).

PLANS FOR THE NEXT PERIOD

1) Develop alternate methods for obtaining crack-free slides. One possibility is annealing of the slides in dry O_2.
2) Make further study of the LiCl-KCl melt and the Li_2SO_4-K_2SO_4 melt.
3) Instead of $NaNO_3$, we will try salt mixtures like Na_2SO_4-$NaNO_3$, which will be more stable at higher temperatures.
4) Vary the index profiles of channel guides by changing the temperature and time parameters of Li_2SO_4-Na_2SO_4 processed slides.
5) Initiate dip coating of thick guides on SiO_2 plates, using a melt of B_2O_3, NaO_2, PbO, SiO_2.
6) Make another attempt to fabricate a low stress waveguide layer on SiO_2 with conventional CVD process.
7) Complete optical measurements on fabricated devices.
8) Examine feasibility of a ray tracing computer program for a layered refractive index structure.

SECTION 4

R&D PERIOD, 1 DECEMBER 1978 TO 31 JANUARY 1979

This report summarizes the work performed during the period from 1 December 1978 to 31 January 1979 on Contract F19628-78-C-0201 entitled "Fiber Optic Couplers". The report is divided into four sections. These are: 1) Theoretical Design Analysis, 2) Planar Coupler Processing, 3) Optical Measurements and 4) Plan for the Next Period.

THEORETICAL DESIGN ANALYSIS

During the previous periods we described a ray tracing procedure for designing planar star and Y couplers. As many as 10,000 rays were launched and tracked through a planar structure during the computer program. For ease of calculation, the planar waveguide structure was assumed to have a step index profile. We have designed an eight-port transmission star coupler and two different Y couplers with the ray tracing program, assuming the step index profile. The computer program determined the number of rays partitioned into each exit port as the parameters (angles, length and width) of the planar structures were changed. The numbers of lost rays were also determined.

During this period we examined the possibility for modifying the computer program where we considered an asymmetric graded index profile (instead of a step index profile) for the planar structure. Such a profile results from a single ion exchange process. We have computed the throughput power due to coupling a graded index fiber to graded parallel channel to graded index fiber. This theoretical result serves as a guideline for evaluating couplers fabricated by the single ion exchange process.

The assumptions and procedures used in the computer program are described below:

The ion exchanged waveguide has been modeled as a stepwise graded index structure consisting of 20 approximately elliptically shaped layers, each layer differing in refractive index. The refractive index varies linearly with layer depth from 1.532 at the ion exchange interface to 1.523 at the deepest layer. The length of the minor axis of an elliptical layer is taken to be twice the channel depth of that layer. The length of the major axis of each of the elliptical layer is set equal to the opening of the photomask (40 μm) plus the length of the mirror axis. The largest ellipse has a minor axis equal to twice the maximum waveguide depth.

The graded index fiber to which we couple the planar structure is assumed to have the following properties, as a source of rays to the planar structure:

1) ray density over the core surface is uniform,

2) the maximum angular spread of the rays varies from the maximum guide numerical aperture at the center of the core NA(0) to zero spread at the core edge, in accordance with the formula

$$NA(r) = (1 - \alpha r^2)\ NA(0),$$

where r is the radial distance from the center of the core. The fiber NA(0) is assumed to be 0.2.

The results of the calculations are shown in Figure 1 where the coupled output power is graphed as a function of the relative position of the fiber to the planar channel. The upper two curves describe the fractional power at the exit (right) end of the channel due to radiation coupled from the fiber. The dotted line represents the output for a channel depth of three core radii, and the continuous line the output for a depth of two core radii. The maxima occurs when the ratio of the core center to surface distance ÷ core radius is unity, i.e., when the upper surface of the fiber core is at the same level as the channel surface.

The lower two curves of Figure 1 show the power coupled from the graded index fiber to the channel and then to the output fiber to the right. The upper continuous curve shows the output when the planar channel is two core radii deep, the dotted curve the output for a channel three core radii deep. The results suggest that the channel depth should be less than or equal to the core diameter for maximum power throughput. The maxima of the upper curve occurs when the upper surface of the core is slightly above the planar surface; approximately 55% of the input light should then be captured in the modes of the exit fiber.

PLANAR COUPLER PROCESSING

During this reporting period we examined the star coupler fabrication process in further detail to determine sources of losses. The result has been an improvement in the quality of the star couplers. First, we determined that, for previous fabrications, the temperature controller for the Li_2SO_4-K_2SO_4 melt was not properly calibrated, yielding a 20°C higher temperature than indicated. The higher temperature tends to corrode the Al masks more readily resulting in poorly formed guides. The temperature controller was recalibrated. Secondly, we have changed from negative to positive photoresists, using a dark field mask.

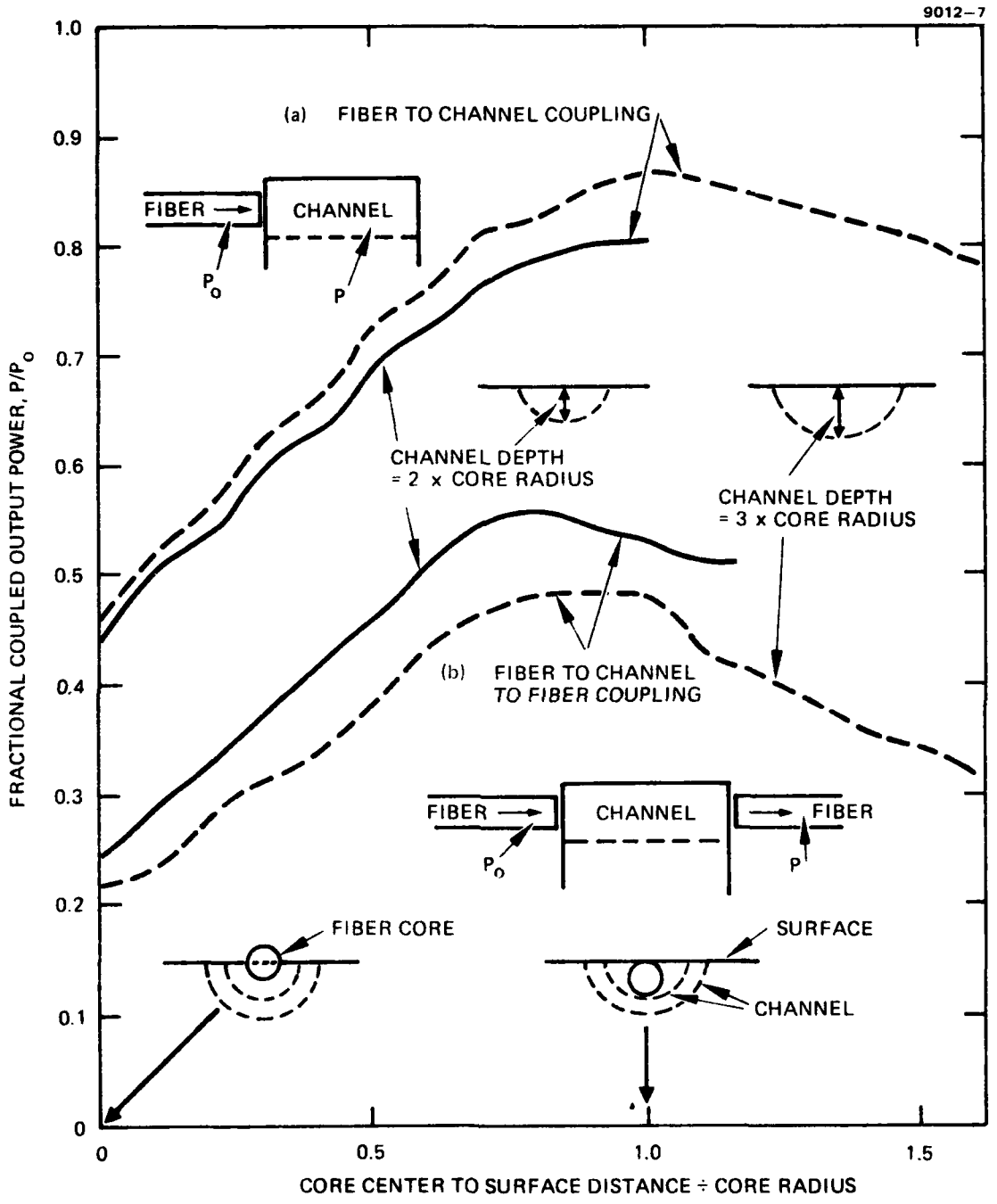

Figure 1. Calculated power throughput for (a) fiber to channel coupling and (b) fiber to channel to fiber coupling, using graded index parallel channel and graded index fiber. Fiber radius = 31.25 μm; channel ΔM = 0.009; graded index fiber NA = 0.2; 40 μm mask opening.

The photoresist is now dipcoated, resulting in more uniform layer of photoresist on the aluminum and therefore more uniform etching. (Previously, spin coating of resist on the long samples resulted in a wavy, non-uniform photoresist layer). The result has been a clean aluminum mask formation on the glass. More importantly, the use of positive photoresist process has eliminated the polymerized photoresist which remains on the aluminum surface with the negative resist process. It is possible that during previous processing the polymerized photoresist had decomposed into products obscuring the star channels and resulting in incomplete ion exchange.

We fabricated two sets of 8x8 transmission star couplers during this period, one set with negative resist and one set with positive resist. Various temperatures and ion exchange immersion times were used. The results were dramatically different. The negative resist couplers exhibited poor light transmission whereas the positive resist process resulted in the best star coupler fabricated to date with throughput better than -10 dB.

During this period we successfully fabricated several ribbons of eight fibers for mating with the 8x8 planar star couplers. The fibers were spaced with etched silicon channels and epoxied into place; the end of the unit was then ground and polished. Figure 2 shows the end view of the ribbon of eight fibers. Figure 3 shows the ribbon of eight fibers epoxied to an 8-port star coupler.

OPTICAL MEASUREMENTS

The last set of ten transmission star couplers fabricated with the positive resist process has yielded the best quality stars thus far, with relatively low surface scattering. Plates containing the stars were immersed in the Li_2SO_4- K_2SO_4 melt for the following temperature and time intervals: 605^oC, 5 min; 605^oC, 10 min.; 605^oC, 15 min; 585^oC, 20 min; 585^o, 40 min. Two stars were located on each plate. The plate immersed for 20 min. at 585^oC appeared to yield the best stars. Fairly clean near field output pattern is observed when light from a fiber is imputted into any of the entrance ports. With light from a fiber ($\sim$200 μW) inputted into one of the entrance ports the sum total power intercepted by a fiber placed in sequence at the 8 exit port was $\sim$20 μW (-10dB) with a maximum of $\sim$24 μW (-9.2dB). There are still considerable

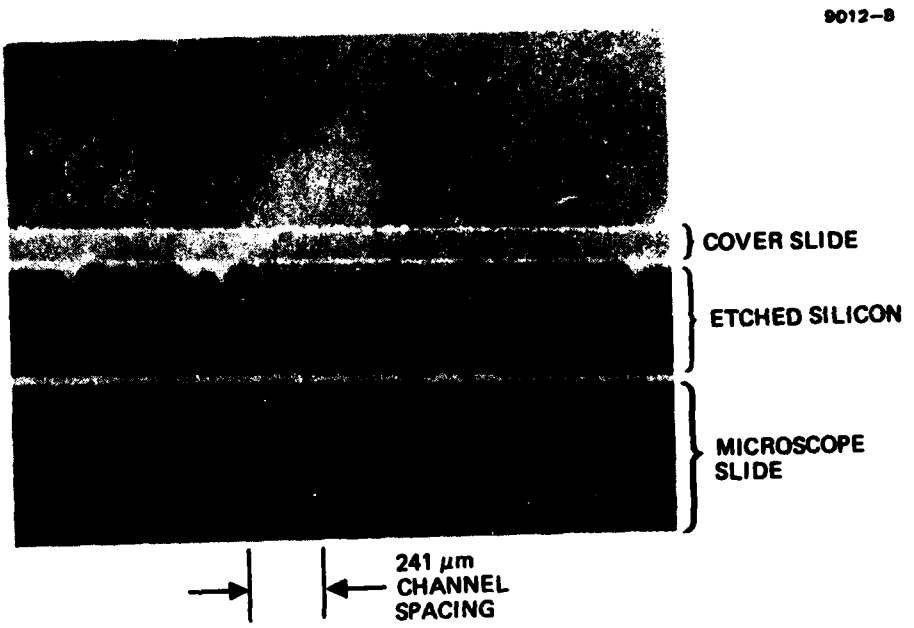

Figure 2. End view of ribbon of light fibers epoxied in etched silicon spacers.

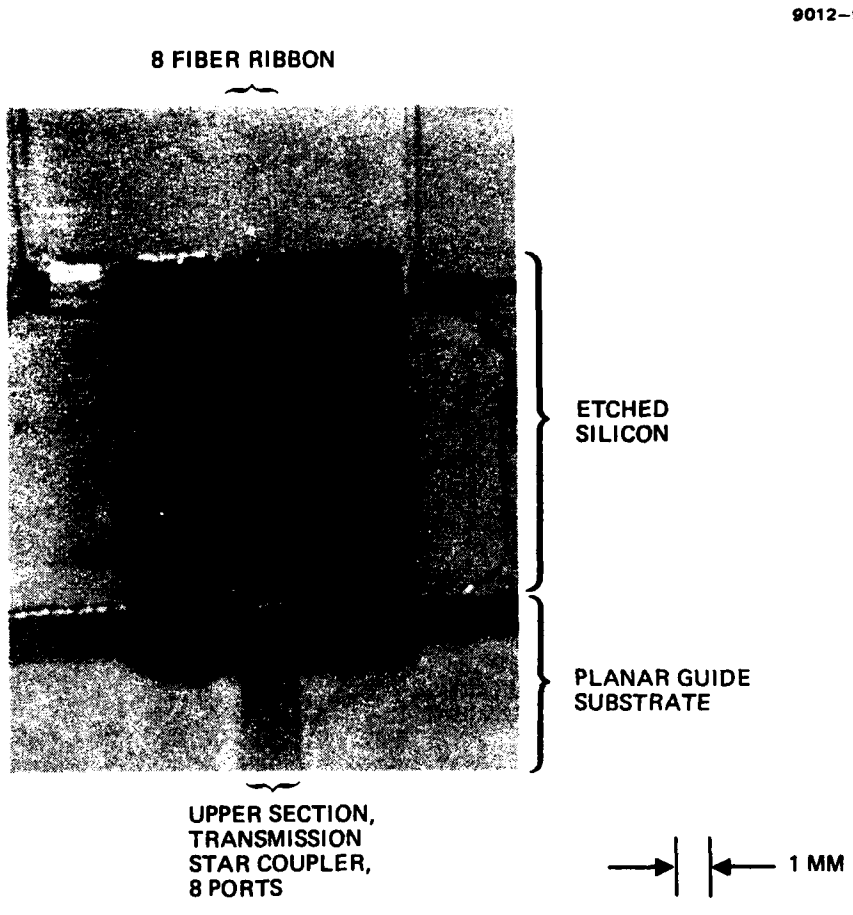

Figure 3. Top view, 8 fiber ribbon epoxied to 8 port transmission star coupler.

variations in the outputs of the 8 exit ports, varying at best by a factor of three. The variations may be due to imperfection scattering and/or lack of sufficient mixing lengths for the graded index structure. The cause of these variations will be investigated further.

We have attached eight fiber ribbons to each end of a transmission star as in Fig. 3 with epoxy. Inputting ∿200 μW into each of the input fibers has resulted in an average sum total output of ∿18 μW. Essentially the same results have been obtained with the ribbons as with the single fiber probe. These measurements will be continued and described more fully in the next report.

We have determined that our ion exchanged channel surfaces are depressed below the adjoining substrate surface, in conflict with a published report. Mechanical probing of the device surface show that the channels and areas exposed to the high temperature melt are depressed approximately 1 μm below the adjacent unexposed surfaces. This result is of importance if further surface polishing is required, subsequent to ion exchange, to remove surface scattering sites.

PLANS FOR NEXT PERIOD

1) To form "buried" channel structures by mating two separate matching planar devices, as suggested by Fig. 4. Experiments will be performed to attach two matching substrates by adhesives, liquids plus pressure, and high temperature fusing. Potential problem areas are substrate curvatures, surface imperfections and channel surface depression rising from ion exchange.

2) To continue ion exchange studies with Li_2SO_4 -Na_2SO_4, LiCl - KCland Na_2SO_4 - $NaNO_3$ mixture. To study double exchange "buried" channels further.

3) To study ray tracing computer program for graded channel Y and star couplers.

4) To continue optical measurements of fabricated devices.

5) To experiment with dip-coated guides and CVD guides on SiO_2 plates.

9012-10

MATCHING CHANNELS
ON SEPARATE GLASS
SUBSTRATES

9012-11

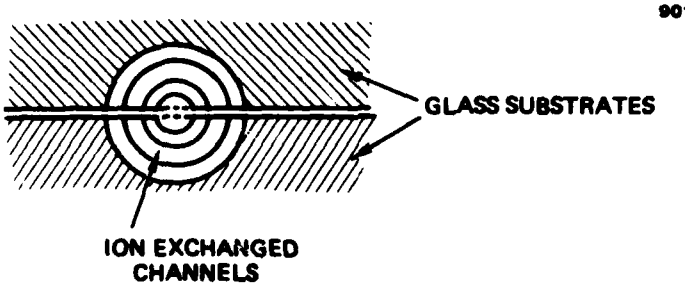

Figure 4. Nearly symmetric graded channels (for coupling to graded fibers) by matching ion exchanged channels on separate glass substrates.

SECTION 5

R&D PERIOD, 1 FEBRUARY 1979 TO 31 MARCH 1979

This report summarizes the work performed during the period from 1 February 1979 to 31 March 1979 on Contract F19628-78-C-0201 entitled "Fiber Optic Couplers". The report is divided into three sections. These are: 1) Buried Channel Experiments, 2) Measured Transmission Star Throughput, 3) Plan for the Next Period.

"BURIED" CHANNEL EXPERIMENTS

Experiments were initiated to fabricate "buried" planar star couplers by laminating two ion-exchanged planar stars, as shown schematically in Fig. 1. As described in previous reports, ion-exchange diffusion results in a graded index waveguide, with the highest refractive index at the exposed planar surface. The constant refractive index profile of a cross-section of a narrow channel waveguide is thus nearly a semicircle. By laminating two planar stars, with the input and output port channels precisely registered, a "buried" channel star coupler with nearly circularly symmetric graded-index profile at the entrance and exit ports can be fabricated. Such a "buried" channel can couple radiation more efficiently to and from a graded index fiber of similar index profile, thereby reducing the excess loss of such a coupler.

We noted previously that potential problem areas in fabricating "buried" channels by lamination are channel surface depression, surface imperfections and substrate distortion or curvature. Our measurements have shown that the ion exchanged channel surface is depressed $\sim$ 1 to 2 microns below the adjoining surface. By grinding and polishing the surface after ion exchange, we are able to smooth the surfaces before lamination. Unfortunately, the glass substrates are seriously distorted, resulting in non-uniform grinding and polishing of the surface. Before proceeding further with the lamination process, we performed experiments to determine the source of substrate distortion and then developed a procedure to minimize the distortion.

Substrate distortion appears to result from Li^+-ion replacement of the Na^+-ion of the glass and not from temperature gradients in the substrate during heating and cooling. We have noted in previous ion-exchanged glass that the surface with the Al-mask has a convex curvature. To determine whether the curvature arise from temperature

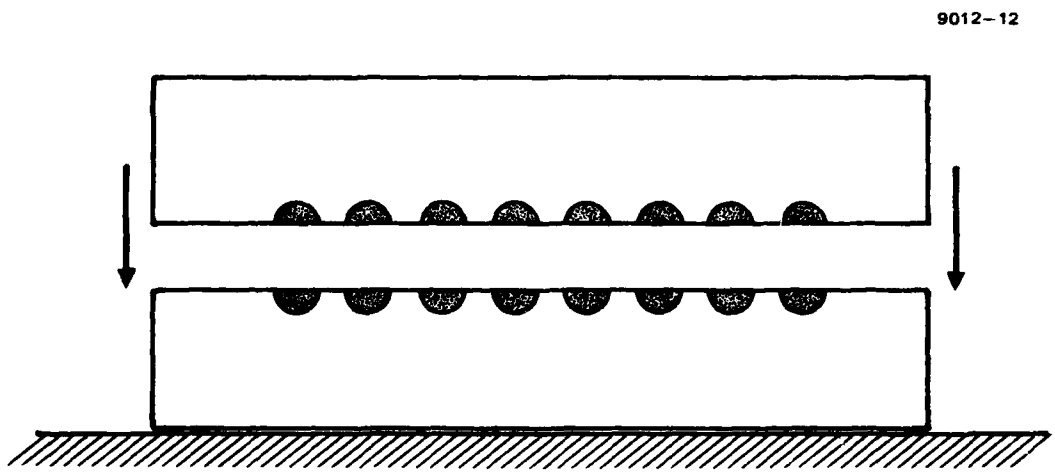

Figure 1. Schematic for forming a laminate of two planar guides to fabricate a "buried" channel coupler.

gradients during cooling due principally to Aℓ on one surface, or from the ion-exchange, the following experiment was performed. A microscope slide was coated with Aℓ, as shown in Fig. 2a, and then immersed in the melt. We observed a definite distortion of the slide while the slide was in the melt after several hours of immersion. No temperature change takes place while the slide is in the melt. The Aℓ surface was noted to be convex. After 120 hours of immersion the microscope slide appeared as shown in Fig. 2a. We conclude that the substrate distortion arises from the Li^+-ion replacement in the glass. The smaller size of the Li^+-ion (0.60Å) compared to that of the Na^+-ion (0.95Å) and possibly tighter coordination with the surrounding silicate ions evidently result in smaller volume for the Li-enriched glass.

After determining that the bending forces arise from the ion exchange, we were able to fabricate undistorted planar stars by symmetrically masking <u>both</u> surfaces of a glass plate. Equal tensions induced on opposite surfaces of the substrate by ion exchange now prevents curving of the substrate. With this technique we have been able to fabricate two sets of stars (three on a plate) with plate curvature limited to <0.1 mm over a 12 cm plate length. These planar stars are now being optically prepared for further "buried" channel experiments.

During this period we also attempted to fabricate laminated "buried" channels by cementing together a pair of existing planar stars. A very thin coat of optically clear epoxy was applied to an interface and the two layers were laminated under pressure. These initial attempts were not successful. The epoxy itself appeared to form a waveguide, guiding light away from the channels. Subsequently, we found that the refractive index of the epoxy was ∿ 1.55, compared to ∿ 1.53 of the glass waveguide. Thus, the thin epoxy layer formed a waveguide itself (of poor quality).

We are continuing to examine other cementing techniques. Since we will now be able to fabricate planar stars with negligible curvatures, uniform grinding and polishing of the surface will be possible. We expect to be able to laminate these surfaces by contact to form "buried" channels, by applying pressure and then cementing the edges of the substrate. We will continue these experiments during the next period.

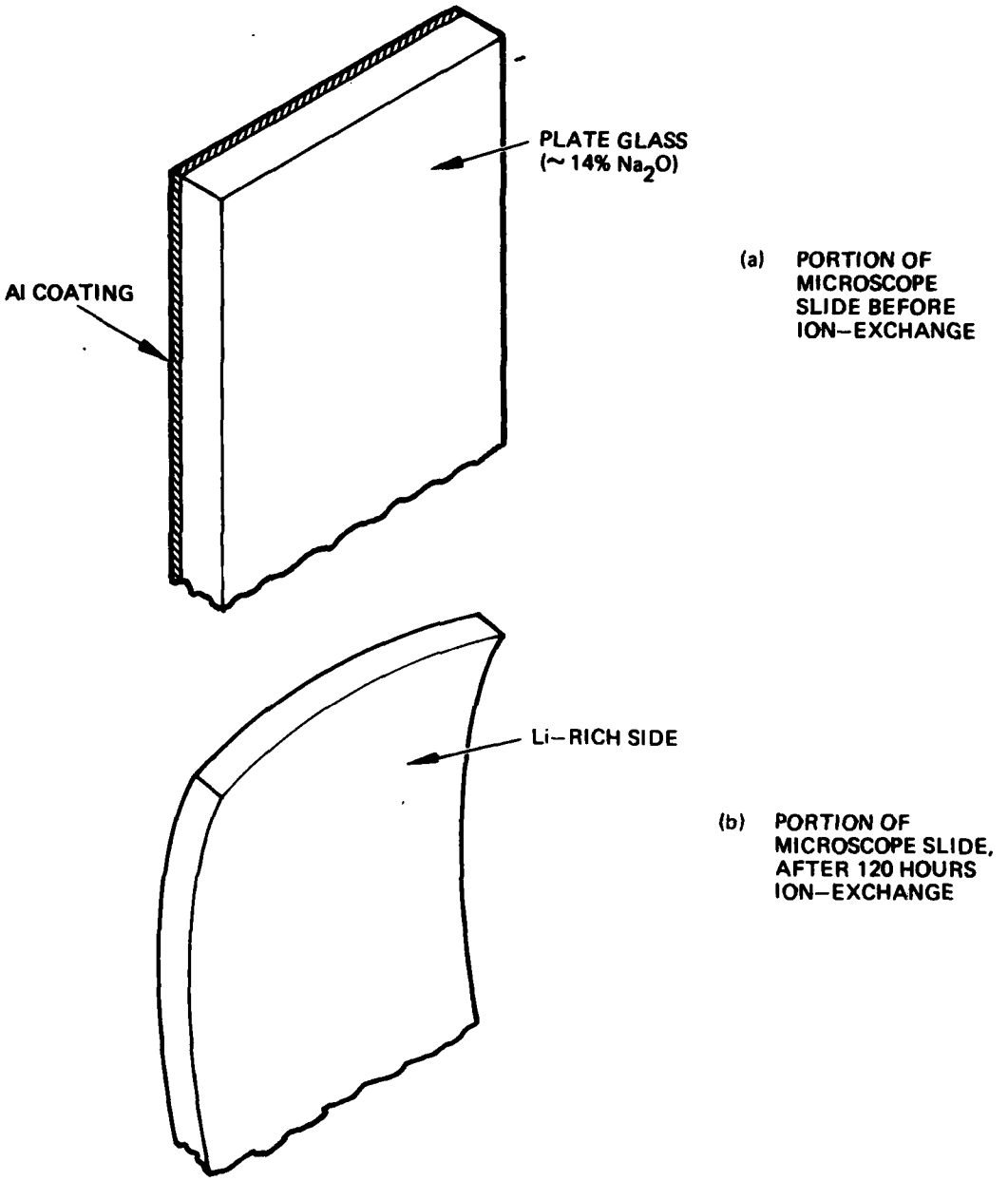

Figure 2. Bending of microscope slide after ion exchange. (a) before exchange, (b) after ∿120 hours of ion exchange at 585°C.

Thermal fusing to form a laminated, buried channel star appears to be promising. During this period we experimented with window plate glass to determine appropriate temperatures and pressures for uniformly fusing the broad faces of one inch squares of glass to one another. A temperature of ∿ 700°C for 5 minutes with no weight (or ∿ 0.5 lb.) on the upper square resulted in uniform contact and fusing across the faces with only slight flattening of the square plates. We found that when the temperture was raised to 750°C, considerable flattening of the squares occurred. Temperatures below 700°C but with larger loading should also result in appropriate lamination of the squares. During the next period experiments to thermally fuse a pair of planar stars will be attempted.

MEASURED TRANSMISSION STAR THROUGHPUT

The measured throughput matrices of a transmission star coupler with 8 input fibers and 8 output fibers cemented in place are given here. There are preliminary results and do not represent the ultimately expected performance.

As mentioned previously, the last set of ten transmission star couplers fabricated with the positive resist process has yielded the best quality stars thus far, with relatively low surface scattering. Plates containing the stars were immersed in the Li_2SO_4-K_2SO_4 melt for the following temperature and time intervals: 605°C, 5 min.; 605°C, 10 min.; 605°C, 15 min.; 585°C, 20 min.; 585°C, 40 min. Two stars were located on each plate. The plate immersed for 20 min. at 585°C appeared to yield the best stars. Fairly clean near field output pattern is observed when light from a fiber is inputted into any of the entrance ports. With light from a fiber (∿ 200 μW) inputted into any of the entrance ports, the maximum sum total power intercepted by a fiber placed in sequence at the eight exit port was 24 μW (-9.2 dB). There are still considerable variations in the outputs of the eight exit ports, varying at best by a factor of three. The variations may be due to imperfection scattering, graded index structure boundaries, and/or lack of sufficient mixing lengths for the graded index structure. The cause of these variations is presently under investigation.

We attached an eight-fiber ribbon to each end of a transmission star (ion exchange process, 585°C for 20 minutes) with epoxy as described previously. During the attachment process, while the epoxy was still liquid, we have observed an increase in the throughput to as much as 28 μW (-8.5 dB). Part of this increase can be assigned to the elimination of the air gap; as the epoxy hardens, however, a slight decrease (∿ 5 to 10%) of throughput power is usually observed. Whether the decrease results from refractive index change of the hardened epoxy or from slight misalignment of the ribbon-to-channel connection as the epoxy hardens is not known at this time.

The 8 by 8 matrices shown in Table Ia represent the distribution of light from each input fiber to each of the output fibers for the ribbon-star-ribbon assembly prior to assembly in a breadboard box. The channels are numbered according to Figure 3. Table 1a shows the initial distribution matrix; Table 1b shows the distribution where the input and output are interchanged. The maximum total throughput of Table 1a is again 24 μW (-9.2 dB), where the power in the input fiber is ∿ 200 μW. The average total throughput is 18.1 μW (-10.4 dB). We note that one of the output channels is much lower than the average distribution, particularly with input into channels #1 and #8. We do not know the reason for this behavior at this time. It appears that a modification of the outer boundaries of the star, to compensate for the graded index of the mixing region, may correct the low output of the channel. The computer program for the graded index star is expected to clarify the result.

The lower matrix (with interchanged input and output) shows total outputs lower (∿ -1 to -2 dB) than the upper matrix. At this research stage, we do not believe that this is significant. The stars were ion-exchanged in a vertical oven with possible thermal gradients in the melt. Inhomogeneous ion exchange could have resulted. Future stars are expected to show uniform reciprocal distributions as the process is improved.

The 8x8 distribution matrices of the planar star coupler assembled in a box with sixteen fiber connectors and sixteen pigtails was measured and is given in Table IIa, and with input and output

TABLE Ia. DISTRIBUTION MATRIX FOR 8x8 PLANAR TRANSMISSION STAR #1, WITH 2 SETS OF FIBER RIBBONS

OUTPUT #2 end / INPUT #1 end	1	2	3	4	5	6	7	8	Total Power μW
1	2.46	1.60	2.26	1.01	3.78	5.99	5.14	0.57	22.31
2	3.30	3.26	2.48	5.41	1.59	4.05	2.68	1.45	24.22
3	0.60	0.92	1.65	3.22	4.30	2.43	2.33	1.79	17.24
4	0.40	0.46	0.58	0.97	2.72	4.56	3.23	3.49	16.41
5	2.53	1.90	2.02	1.15	1.68	1.80	1.75	2.66	15.49
6	1.70	2.03	1.98	1.12	1.76	1.67	2.46	2.79	15.51
7	6.87	3.06	1.38	1.33	1.20	1.23	0.90	0.97	16.94
8	0.70	6.90	3.05	1.30	1.14	0.93	0.96	1.34	16.32
								Avg.	18.1 μW

TABLE Ib. SAME AS Ia, EXCEPT INPUT AND OUTPUT ARE REVERSED.

OUTPUT #1 end / INPUT #2 end	1	2	3	4	5	6	7	8	
1	3.59	2.38	0.85	0.54	1.48	1.24	1.77	0.68	12.55
2	3.29	3.18	0.86	0.69	1.00	1.68	0.85	1.45	13.0
3	3.20	3.61	1.42	0.37	0.52	0.78	0.56	0.67	11.13
4	2.50	4.60	3.25	0.64	0.30	0.51	0.63	0.69	13.12
5	10.70	2.50	1.81	1.38	0.55	0.82	0.40	0.46	18.62
6	3.49	5.00	1.43	1.42	0.72	0.88	0.41	0.36	13.71
7	2.37	2.33	1.49	0.56	1.28	1.75	0.47	0.33	10.58
8	0.35	2.30	0.98	2.78	2.51	1.39	0.72	0.50	11.53
								Avg.	13.03

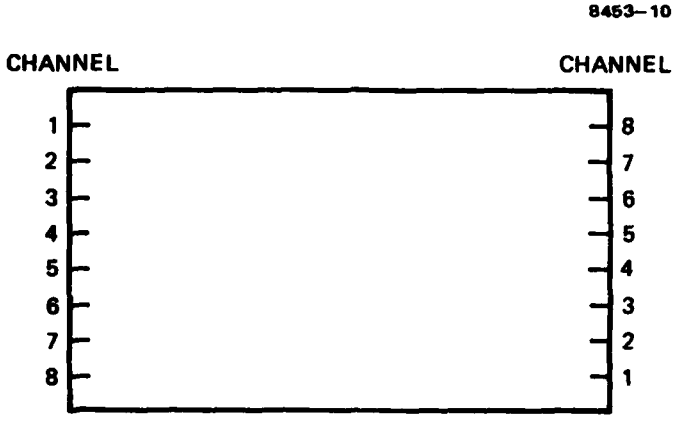

Figure 3. Numbering of the channels of the transmission star coupler.

TABLE IIa. DISTRIBUTION MATRIX FOR STAR #1, BREADBOARDED IN A BOX, WITH FIBER CONNECTORS

output (white dot end) / input	1	2	3	4	5	6	7	8	Total µW Sum Measurement	
1	1.6	1.3	1.6	1.3	2.5	2.5	2.8	.50	14.1	14.40
2	1.6	1.5	1.5	3.7	1.1	2.9	1.6	1.0	14.9	15.60
3	.52	1.1	2.0	3.2	3.2	1.5	1.2	1.2	13.9	13.23
4	.33	.33	.46	.58	1.8	1.9	1.5	1.8	8.7	8.70
5	1.6	1.3	1.0	.91	1.3	1.4	1.3	1.8	10.6	10.93
6	1.0	1.1	.80	.56	.91	1.6	.96	1.6	8.5	9.87
7	2.0	1.7	.62	.91	.60	.41	.42	.45	7.1	7.65
8	.50	2.7	1.2	.60	.77	.42	.50	.80	7.5	8.20
							Avg.		10.7	11.1

TABLE IIb. SAME AS IIa EXCEPT INPUT AND OUTPUT REVERSED

output / input (white dot end)	1	2	3	4	5	6	7	8	Total µW Sum Measurement	
1	1.6	1.6	.57	.36	2.0	.67	2.0	.73	9.5	10.36
2	.85	1.4	.70	.26	.33	.60	.54	.67	5.4	6.50
3	2.1	1.9	1.3	.42	.59	.65	.22	1.0	8.2	8.93
4	.72	.9	1.7	.26	.47	.40	.32	.52	6.3	6.42
5	2.7	1.5	2.1	.81	.53	.57	.24	.40	8.9	9.45
6	1.2	2.6	.90	1.2	.86	.58	.22	.20	7.8	8.50
7	.93	6.1	6.3	.90	1.3	.68	.15	.22	6.6	8.20
8	.13	1.4	.93	2.3	1.74	.47	.38	.30	7.7	8.02
							Avg.		7.6	8.5

reversed in Table IIb. We recall that the matrix of Tables Ia, b is that for the star with ribbon pigtails, that of Table IIa, b, the same star plus ribbon, but with eight input and eight output fiber connectors. The average loss due to the two connectors is $\sim$ 2.3 dB, or a loss of -1.2 dB per connector.

We wish to note that the matrix measurements of the boxed star were sensitive to movement of certain of the input pigtails and to launch conditions of the laser light. Whether this problem arises from distortion at the connector is not clear at this time, but the effect will be examined more fully and corrected.

The highest throughput was down $\sim$ -9 dB relative to the power in the input fiber. We can partition the loss as follows:

Measured Insertion Loss	=	Measured Coupling Loss	+	Estimated Propagation Loss	+	Estimated Internal Loss

or

$$9 \text{ dB} = 4.2 \text{ dB} + \left(0.1 \frac{\text{dB}}{\text{cm}}\right) (8 \text{ cm}) + [4.0 \text{ dB}]$$

The measured coupling loss of 4.2 dB was determined from the experiments with parallel channels described previously. The remainder of the insertion loss is partitioned to propagation loss and the internal loss of the star structure. If the propagation loss is taken to be very small (0.1 dB/cm), an estimated internal loss of 4.0 dB remains. The latter loss may be compared with the packing fraction loss of 3.8 dB for a linear array of fiber. We expect that the fiber to star coupling loss can be reduced to < 1 dB with proper matching of index profiles, thereby resulting in an insertion loss of $\sim$ 5-6 dB.

PLAN FOR THE NEXT PERIOD

1) To continue the effort to form "buried" channel star couplers by laminating two matching planar structures, using both adhesives and high temperature fusing.

2) To experiment with dip-coated wave-guides and CVD wave-guides on SiO_2 and glass plates.

3) To continue further ion exchange studies and to continue experiments to-from "buried" channels with double ion-exchange.

4) To continue ray tracing program for graded index couplers.

MISSION
of
Rome Air Development Center

RADC plans and executes research, development, test and selected acquisition programs in support of Command, Control Communications and Intelligence (C^3I) activities. Technical and engineering support within areas of technical competence is provided to ESD Program Offices (POs) and other ESD elements. The principal technical mission areas are communications, electromagnetic guidance and control, surveillance of ground and aerospace objects, intelligence data collection and handling, information system technology, ionospheric propagation, solid state sciences, microwave physics and electronic reliability, maintainability and compatibility.

Printed by
United States Air Force
Hanscom AFB, Mass. 01731